

**DESIGN AND CONTROL OF A SOAKING
STATION AND ASSOCIATED ACCESSORIES FOR
HIP IMPLANT WEAR TEST SIMULATOR**

**A Thesis Submitted to
the Graduate School of
İzmir Institute of Technology
in Partial Fulfillment of Requirements for the Degree of
MASTER OF SCIENCE
in Mechanical Engineering**

**by
Doruk SEVÜK**

**October 2024
İZMİR**

We approve the thesis of **Doruk SEVÜK**

Examining Committee Members

Assoc. Prof. Dr. Şenay MİHÇİN

Department of Mechanical Engineering, İzmir Institute of Technology

Prof. Dr. Serhan ÖZDEMİR

Department of Mechanical Engineering, İzmir Institute of Technology

Prof. Dr. Şeniz ERTUĞRUL

Department of Mechatronics Engineering, İzmir University of Economics

08 October 2024

Assoc. Prof. Dr. Şenay MİHÇİN

Supervisor, Department of
Mechanical Engineering, İzmir
Institute of Technology

Prof. Dr. M. İ. Can DEDE

Head of the Department of
Mechanical Engineering

Prof. Dr. Mehtap EANES

Dean of the Graduate School

ACKNOWLEDGEMENTS

My heartfelt appreciation goes to my advisor, Associate Professor Dr. Şenay MİHÇİN, for the valuable technical support and motivational consultancy throughout my master's thesis. Above all, special thanks are extended for accepting me in a research group and bringing out valuable contributions that have helped develop me as a person and professionally. It has been a great privilege to work under her mentorship, and I feel so lucky to be able to learn from her.

I would like to extend my special thanks to my family for their great support during my schooling. Their belief and encouragement, in turn, build me up with strength and inspiration.

In this regard, I would like to extend my sincerest thanks to all members of the Biomechanics and Motion Capture Laboratory at IZTECH, who created a very positive, collaborative working environment that really enhanced my research experience. I would also like to thank my colleagues Mehmet YILMAZ and Ahmet Mert ŞAHİN for the valuable comments, technical support in the experimental part of my studies, and friendships developed.

I am grateful to TUBITAK, as the realization of this research was possible at the Izmir Institute of Technology within the framework of the TUBITAK 2232 Funding Scheme (Project Number: 118C188) and the AUDP project (2022IYTE-3-0019). Without their support, it would not be possible to carry out this research.

I am also grateful to ÇOLBAN Elektrik Otomasyon, Hidropar İzmir, and Hidropar HKTM for their willing support. I am also thankful to Mitsubishi for giving me many aspects to solve problems.

ABSTRACT

DESIGN AND CONTROL OF A SOAKING STATION AND ASSOCIATED ACCESSORIES FOR HIP IMPLANT WEAR TEST SIMULATOR

This thesis focuses on the design validation and control of a soaking station and associated accessories of the hip implant wear test simulator. In fact, the soaking station itself is an accessory device to the 4 Degrees of Freedom (DoF) hip simulator, simulating the dynamic wear phenomena.¹ The intended use of the soaking station is to apply compressive force simultaneously, with the hip implant wear simulator, subjected to the same environmental conditions. The same environmental conditions are maintained through the associated accessory devices that are used for controlling the temperature and flow of the serum liquid.^{2,3} The soaking station performs a compressive force cycle and fluid uptake by soaking the hip implant in serum liquid, creating a static simulation environment. The soaking station provides a comparative wear result, making possible gravimetric analysis of wear results. Testing of hip implants before clinical applications requires testing according to the ISO 14242 hip wear test standards.⁴ After justifying that both machines can be simulated according to ISO standards, it is aimed to design a soaking station to compare the results with the hip joint wear test simulator based on the Muslim praying and daily life activities of Turkish people.⁵ Thus, this thesis can advance the knowledge about hip implant wear mechanisms and provide improvements in the design and control of local implant wear simulator systems. A comprehensive literature review, discussion of control and validation of the hip wear simulator, and the soaking station form the scope of this thesis.

Keywords: *Hip prosthesis, wear analysis, axial force, static simulation, dynamic simulation, ISO 14242, synovial fluid, programmable logic controller, gravimetric analysis, machine design*

ÖZET

KALÇA İMPLANTI AŞINMA TEST SİMÜLATÖRÜ İÇİN ISLATMA İSTASYONUNUN VE İLGİLİ AKSESUARLARIN TASARIMI VE KONTROLÜ

Bu tez, bir ıslatma istasyonunun ve kalça aşınma testi simülatörünün ilgili aksesuarlarının tasarım doğrulaması ve kontrolüne odaklanmaktadır. Aslında, ıslatma istasyonunun kendisi, dinamik aşınma olaylarını benzetim eden 4 Serbestlik Derecesi kalça simülatörüne bir aksesuar cihazdır.¹ Islatma istasyonunun amaçlanan kullanımı, aynı çevre koşullarına tabi tutulan kalça implantı aşınma simülatörü ile aynı anda basınç kuvveti uygulamaktır. Aynı çevresel koşullar, serum sıvısının sıcaklığını ve akışını kontrol etmek için kullanılan ilişkili aksesuar cihazları aracılığıyla korunur.^{2,3} Islatma istasyonu, kalça implantını serum sıvısına batırarak bir basınç kuvveti döngüsü ve sıvı alımı gerçekleştirir ve statik benzetim ortamı yaratır. Islatma istasyonu, karşılaştırmalı bir aşınma sonucu sağlayarak aşınma sonuçlarının gravimetrik analizini mümkün kılar. Klinik uygulamalardan önce kalça implantlarının test edilmesi, ISO 14242 kalça aşınma test standartlarına göre test edilmesini gerektirir.⁴ Her iki makinenin de ISO standartlarına göre benzetim edilebileceğini kanıtladıktan sonra, sonuçları Türk halkının Müslüman ibadet ve günlük yaşam aktivitelerine dayalı kalça eklemi aşınma test simülatörü ile karşılaştırmak için bir ıslatma istasyonu tasarlanması amaçlanmaktadır.⁵ Bu nedenle, bu tez kalça implantı aşınma mekanizmaları hakkındaki bilgiyi iletilebilir ve yerel implant aşınma simülatörü sistemlerinin tasarımı ve kontrolünde iyileştirmeler sağlayabilir. Kapsamlı bir literatür incelemesi, kalça aşınma simülatörünün kontrolü ve geçerliliğinin tartışılması ve ıslatma istasyonu bu tezin kapsamını oluşturmaktadır.

Anahtar Kelimeler: *Kalça protezi, aşınma analizi, eksenel kuvvet, statik benzetim, dinamik benzetim, ISO 14242, sinovyal sıvı, PLC, gravimetrik analiz, makine tasarımı*

TABLE OF CONTENTS

LIST OF FIGURES	vi
LIST OF TABLES.....	ix
LIST OF ABBREVIATIONS.....	x
CHAPTER 1 INTRODUCTION	1
1.1. Aim of Study.....	1
1.2. Introduction of Wear Tests and Control System.....	6
CHAPTER 2 LITERATURE REVIEW	11
CHAPTER 3 METHODOLOGY AND MATERIALS.....	14
3.1. Design and Parameters of Soaking Station.....	14
3.2. Materials and Integration of Accessories.....	22
3.3. Accessories of The Soaking Station	26
3.4. Control and Integration of The System.....	30
3.5. Software Architecture and PLC Programming	34
3.6. Control and Integration of The System.....	41
3.7. Calibration of The Electrode.....	47
CHAPTER 4 RESULTS AND DISCUSSION.....	50
CHAPTER 5 CONCLUSIONS	54
REFERENCES	56

LIST OF FIGURES

<u>Figure</u>	<u>Page</u>
Figure 1. Used Data from New Database on Hip Joint for Daily Life Activities: (a) QS, (b) gait, (c) OBC, (d) STL, (e) SQL, (f) AST, (g) RAI, (h) RTS, (i) SJD, (j), ACS, (k) DCS.	3
Figure 2. Wear Test Control Parameters Flow Chart for Hip Joint Implants.	4
Figure 3. Design of Soaking Station Mechanism.	8
Figure 4. Force Profile According to ISO 14242-1.	17
Figure 5. Electromechanical Cylinder.	18
Figure 6. Soaking Station CAD Design.	19
Figure 7. Manufactured Soaking Station.	20
Figure 8. X-Y Table Assembly.	21
Figure 9. The Individual Components of An Illustrated Total Hip Replacement.	21
Figure 10. Components of The Used Test Specimen.	22
Figure 11. The Coordinate System of The Femoral Head with Jig Design.	22
Figure 12. Integrated Hardware Components with Applied Soaking Station.	23
Figure 13. Used PLC Modules in The Main System of A1: PLC-Temperature Module, CPU: PLC-Main Unit, 1: Digital I/O Module with RELAY OUTPUT, 2: Digital I/O Module with DC INPUT (SINK/SOURCE), 3: Analogue I/O Module, 4: Simple Motion Module, 5: PLC-Network Module.	24
Figure 14. U3 50kN Loadcell.	25
Figure 15. The Peristaltic Pump.	26
Figure 16. Manufactured Thermostat with Thermocouple Inside.	28
Figure 17. (Left) The Thermostat Cad Design and (Right) Individual Parts of The Design.	29
Figure 18. The Peristaltic Pump Used for The Liquid Circulation and The Manufactured Thermostat Assembly.	29
Figure 19. The Manufactured Soaking Station.	30
Figure 20. Physical Representation of The Manufactured Hip Joint Implant Wear Test Simulator and The Soaking Station.	31

<u>Figure</u>	<u>Page</u>
Figure 21. Schematic Representation of Motor Controls for Both Hip Wear Testing Simulator and Soaking Station.	32
Figure 22. The Heated Bovine Serum Fluid Circulation Control for Test Environment.....	33
Figure 23. Test Environment Control Representation	34
Figure 24. Physical Network Environment.....	35
Figure 25. Read Processed Loadcell Data from PLC Ethernet Module.	36
Figure 26. Adjusting PID Settings for Controlling Z-axis.....	36
Figure 27. PID ladder for Z-axis Control.	37
Figure 28. System Blocks of Proximity Sensors and Arranged for Homing Process.	38
Figure 29. Positioning Code on Virtual Motor at System Blocks.	38
Figure 30. Manual Input Screen for Positions and Speed Control.	39
Figure 31. Arranging Master at Axis-8 and Slave at Axis-1/2/3 Synchronous Movement.	39
Figure 32. Degree and Force Data Inputs While Implementing to The PLC.	40
Figure 33. Virtual Tryouts in The PLC program.	40
Figure 34. Fixture for HPR Operation.	41
Figure 35. Representation of Aligning Fixture part X-Y Moving Table and 6-axis Loadcell.	42
Figure 36. Scale Home Position Signal Behavior for Axis 1, 2 and 3.....	43
Figure 37. Home Position of Machine by Using Fixture Part.	44
Figure 38. FARO CMM Robotic Arm.....	45
Figure 39. Proximity Sensors Integrated Behind the Motor Shafts for Axes 1, 2 and 3.....	47
Figure 40. (a) Images of The Electrode Filled with Saturated KCL Electrolysis and (b) The Environment in Which The Electrode Is Kept.....	48
Figure 41. Electrode Calibration Setup.....	49
Figure 42. Measurement for The Electrode Calibration	49
Figure 43. Manual Commutation of The Servo Motors.	50
Figure 44. Cycle Time While System Operating.....	51
Figure 45. Bending Representation for Possible Critical Failure Component.	52

Figure

Page

Figure 46. Maximum Sheer Stress of Critical Part at Soaking Station from
Analysis. 52



LIST OF TABLES

<u>Table</u>	<u>Page</u>
Table 1. ISO-14242-1 Standards Boundary Conditions.	5
Table 2. Maximum Compression Force (Multiplied by 75 kg).....	15
Table 3. YT15 Flow Rate.	27



LIST OF ABBREVIATIONS

<u>Abbreviations</u>	<u>Definition</u>
QS	Qualisys static posture
OBC	Obstacle Crossing
STL	Stoop Lifting
SQL	Squat Lifting
ACS	Ascending Stairs
AST	Asian Style Sitting
RAI	Ruku' and I'Tidal
RTS	Ruku' to Sujud
SJD	Sujud
DCS	Descending Stairs
BCS	Bovine Calf Serum
DoF	Degrees of Freedom
RoM	Range of Motion
EMC	Electromechanical Cylinder
I/E Rotation	Internal/External Rotation
F/E Rotation	Flexion/External Rotation
A/A Rotation	Abduction/Adduction Rotation
SF	Safety Factor
PLC	Programmable Logic Controller
PID	Proportional Integral Derivative
HPR	Home Position Return
SCE	Saturated Calomel Electrode
KCL	Potassium Chloride

CHAPTER 1

INTRODUCTION

The thesis focuses on developing a soaking station and improving implant testing under realistic human body conditions as part of a hip joint wear test simulator. Both systems were manufactured and used within the scope of a TUBITAK 2232 project at Izmir Institute of Technology according to ISO 14242 standards^{2,3}. The soaking station project is also supported for its manufacturing by the AUDP project (2022IYTE-3-0019). Investigating the hip joint implant wear rate requires the measurement of different variables such as the dynamic movements of the hip simulator, the static compressive forces acting on the hip implants, and the fluid absorption in the hip implant. This introduction explains the concept of the soak station, what is intended with it, and how it was developed.

1.1. Aim of Study

Total joint replacement is a common practice applied worldwide when joints lose their functionality. When joints lose their functionality, the standard is joint arthroplasty. Total replacement of the joint, for hip (THR) and knee (THK) are the procedures applied in practice. For THR, the main limitation is a 15-year implant service life, which is unsatisfactory for patients under 60, of which 44% demand a life expectancy of more than 20 years.⁶ Total joint replacements (TJR), being a standard solution; approximately half a million knee and 2 million hip replacements are expected to be performed per year by 2025 because of aging populations worldwide and increasing demand for a higher quality of life.⁷

The current testing implant methodology is based on measuring the material removal rate by the compare of the wear volume of test specimens before and after, which is important to understand longevity and reliability in clinical applications. For that,

physical simulators are prepared to simulate the in-vivo conditions of implants inside the human body.⁸ Boundary conditions for these tests are determined from gait laboratory data on the walking cycle, along with the data on the range of motion considering assumptions about average body weight at the hip joint implant simulator. The gait data is normally adjusted by multiplying the force 2 or 3 times to represent dynamic loading scenarios.^{9,10} The prototype of the implant is subjected to million-cycle repetitions under these boundary conditions to observe the wear rate. The failure and pass criteria are assessed according to predefined test specs. Because it can determine the failure and acceptance criteria.^{2,3,5} If the material removal rate measured is higher than acceptable limits, then the product should fail, and revisions shall be necessary before it goes to production.

This thesis is part of the TUBITAK 2232 research program which aims at developing ‘new generation implants for all. Currently, implants are tested against the gait boundary conditions as mandated by ISO 14242.^{2,3} In this project, to design implants according to the needs of the Eastern lifestyle, data were collected from the Turkish population while they performed daily life activities⁵ 200 people formed an online database. These data were used to calculate the range of motion and associated force values for each intended daily life activity. The project is based on the intended use design. The hip joint implant wear test simulator and the soaking station designs are designed to simulate normal daily activities and some unique motions, such as Muslim praying, Yuga, and Sports such as climbing in Figure 1.^{1,5} The chosen data are collected from the Department of Mechanical Engineering of Izmir Institute of Technology in Izmir, Turkey.⁵

Since implants are designed and tested only against walking criteria, the goal is to understand the boundary conditions of daily life activities and design a soaking station for the hip joint wear test simulator, which can test implants according to these intended daily life activities compared with wear results.¹⁰ Because implants are affected by a liquid environment, they have fluid uptake and are changed as volume in testing. The soaking station applies only static force to test specimens while providing the same warm liquid environmental conditions as the hip joint implant wear test simulator as in Figure 2. Both machines simulate the wear tests on the test specimens by following the same Force/Time data synchronously. In this way, the wear results resulting from static load can be compared with the dynamic wear test results obtained from the hip wear test simulator as a reference unit.⁴

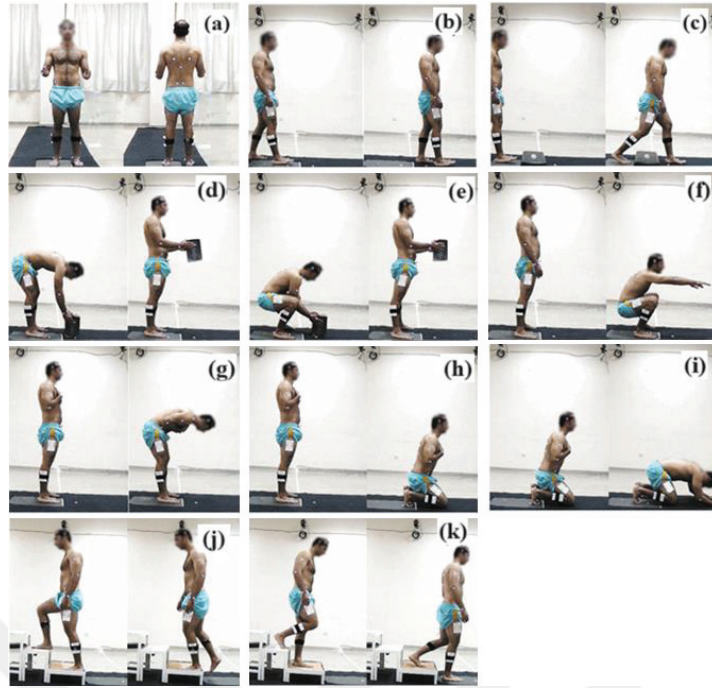


Figure 1: Used Data from New Database on Hip Joint for Daily Life Activities: (a) QS, (b) gait, (c) OBC, (d) STL, (e) SQL, (f) AST, (g) RAI, (h) RTS, (i) SJD, (j), ACS, (k) DCS (Source: 5).

Currently, the best data available for the motion of the lower body is the gait lab data, which are collected in the lab environment, using markers and infrared camera systems at the university under the TUBITAK 2232 project “New Generation Implants for All” with project number 118C188. Wear tests are performed by programming joint reaction forces and range of motion (RoM) data.⁵ Biomechanics is urgently needed to reduce dependency on foreign products, as manufacturers often need to outsource testing to other centers according to ISO standards^{2,3} for CE marking.¹¹ The present project is intended to test hip and even knee joint implants through a programmable range of motion and force values by the hip joint implant wear test simulator and the soaking station that tests their lifespan in general. Based on the test results, new-generation implants that serve the needs of the Turkish population are to be designed, and successful test results can reduce the revision operations in hospitals.^{5,12} The study may increase the research potential for investigating new materials, and coatings to reduce the friction in implants and enhance the research capacity in the field of material science, as well as biomedical engineering in support of medical solutions.¹¹⁻¹³

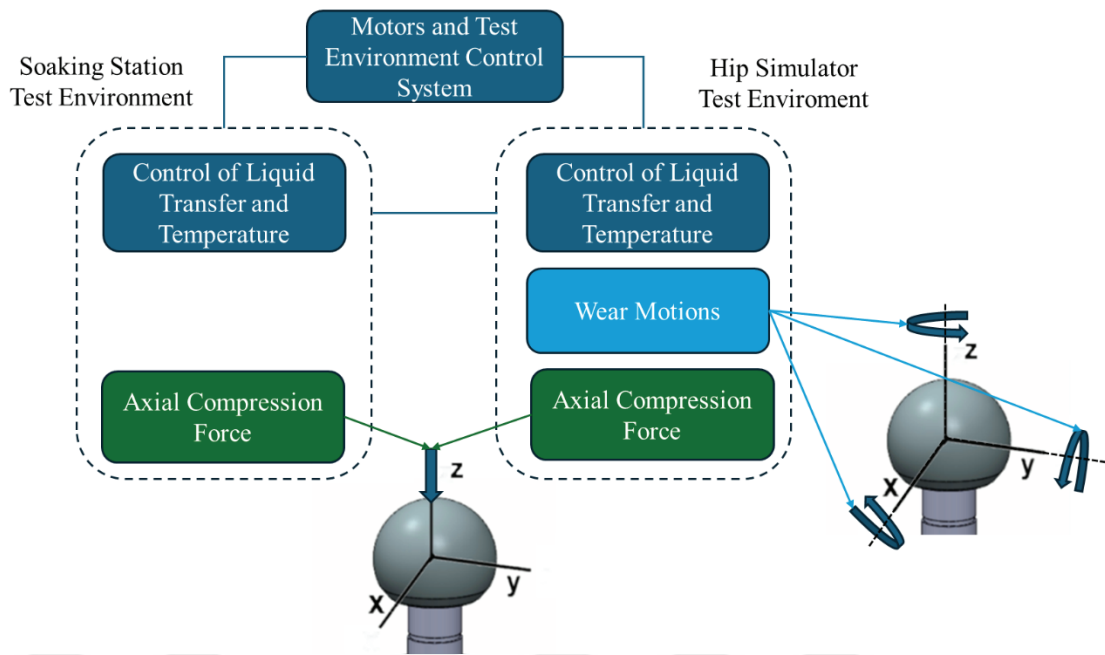


Figure 2: Wear Test Control Parameters Flow Chart for Hip Joint Implants.

In this project, the kinematic data are fed into a computer model, where the joint RoM data and reaction forces can be calculated using computational biomechanical modeling packages in silico simulation.⁵ So, the products can be designed according to the collected RoM data and reaction forces. It provides force/time and angle/time data, then deviation can be measured. These deviations should not exceed 3% of maximum RoM values if the system is to meet the ISO standards shown in Table 1.^{2,3} This means that the system works within quantified boundaries and the implants can be tested for these new boundary conditions. With these new boundary conditions, more realistic simulation results are to be provided to qualify a product according to ISO standards.^{2,3,5}

In this study, it is expected that with these different boundary conditions, different wear patterns over the implants are to be observed. When the boundary conditions resulting from these new activities are applied to the implants, the implant life can be calculated, and more compatible results can be obtained with the surgical data and practical data. According to the obtained wear profile, new implant designs that can be more durable can be suggested. However, the main purpose here is that when the wear percentages of all "daily life activities" data are added within certain ratios, the implant life is expected to be shorter than expected.⁵ This prediction needs to be tested for reality by making simulations on the test specimen using a simulator and a soaking station. Then,

the new implant designs developed under these conditions can be tested, aiming to reduce wear and obtain longer-lasting implants. In this project, the kinematic data are fed into a computer model, where joint RoM data and reaction forces can be calculated using computational biomechanical modeling packages in silico. So, the products can be designed according to the collected RoM data and reaction forces. It provides force/time and angle/time data, then deviation will be measured. It should be within 3% of these input values. There should be a minimum deviation according to ISO standards.^{2,3} It shows that the system can be controlled in these specs.

Table 1: ISO-14242-1 Standards Boundary Conditions.

Parameter	ISO-14242-1
Maximum Force	3 kN \pm 3 %
Frequency	1 Hz \pm 0,1 Hz
Test Fluid	BCS
Temperature	37°C \pm 2 °C
Repeat Test Cycles	5 Million Cycles

With these inputs, new-generation implants are to be tested with these new boundary conditions to be qualified. With these new boundary conditions, more realistic simulation results are to be provided to qualify a product according to ISO standards.^{2,3,5} In this study, it is expected that with these different boundary conditions, different wear patterns over the implants are to be observed. With these newly generated implants, physical simulator results using population-based boundary conditions can be compared with computer simulations for validation. The intention is to reduce the wear volume to qualify these new-generation implants.

1.2. Introduction of Wear Tests and Control System

The soaking station is an integral part of the novel hip wear simulator project and functions as an accessory to hip wear test simulators. Both the hip wear test simulator and the soak station were designed, manufactured, and used at the university. These simulators primarily conduct wear testing of implants according to the walking boundary conditions mandated by ISO 14242-1 and ISO 14242-2 standards.^{2,3} The design of both the hip wear test simulator and the soaking station allows the application of various force data to hip implants and increases testing flexibility. An interactive user interface that can accept flexible force data allows the soaking station to operate according to specifications. The project aims to develop a programmable interface with a flexible database that can integrate data from human daily life activities and personal movement data, rather than a simulator that only works according to ISO standards.⁵ The simulation test parameters of the hip joint are collected from Turkish volunteers during some daily life activities in the university laboratory to ensure that both the hip wear test simulator and the soaking station simulate real-life conditions. The aim is to simulate the wear of the hip joint under these new biomechanical data closer to real-life conditions and thus increase the accuracy of wear loss calculations on test specimens.¹

The Hip Wear Test Simulator and Soaking Station are used to evaluate the durability and performance of hip implants by simulating the kinetic and kinematic values of the hip joint on the test specimen.¹⁴ Hip wear test simulators must specifically comply with ISO 14242 standards. Simulators with examples in the literature show that they allow control of various parameters in the hip joint such as axial load, flexion-extension, abduction-adduction, and internal-external rotation.¹⁵ To determine the fluid absorption of the hip implant, the load movement must be controlled to mimic physiological conditions. Controlling the movement and load on the test specimen ensures that the wear conditions on the hip closely mimic the actual physiological environment. Precise control of the load movements according to the load cycle is required to ensure the accuracy of the wear test results. The purpose of the simulator is to evaluate the linear wear and volumetric wear rates from the components of the test prosthesis by performing the hip joint movements and comparison force on the test specimen.²⁻⁴ To obtain volumetric wear rate results, gravimetric analysis is used to measure wear rate. Gravimetric analysis tests

are performed periodically between 500,000 to 5 million cycles according to ISO 14242 standards.^{2,3}

The soaking station performs a static simulation for the test specimen by applying a compressive force in a liquid environment. This simulation allows the analysis of volume and weight changes caused by the fluid intake of the hip implant components due to the compressive forces and wetting on the test sample.⁴ Before an implant is inserted into the human body and is used in a patient's surgery, it is tested on the hip wear test simulator according to the hip wear test parameters specified in ISO 14242 standards. Currently, hip simulators used in medical testing have control stations that allow simultaneous testing and fluid loading to reference wear rate results. If an implant needs to be tested, the hip implant should be tested in a control station to expose a test specimen to different dynamic wear conditions and joint motion wear compared to this test specimen. The use of a soaking station is used to obtain a second result and compare the amount of wear on the test specimens through the motion cycles of the hip wear simulator.^{2,4,16,17} Also considering the ISO 14242 standards, it is necessary to create a system that meets the mechanical precision requirements of the soaking station that controls the conditions of the single-axis pressure system as well as the human body's environmental conditions.^{2,4,18} A precision linear actuator press system called a soaking station has been developed to meet these requirements. Controlling these two different test specimen environments with specific conditions helps to isolate the wear rate caused by the mechanical friction of the joint movement from individual variables of human body factors that cause the fluid absorption of joints such as fluid temperature, viscosity, and the cyclic weight load on the joint. An accurate comparison of wear can be made by comparing the wear results of the given motion cycles in the hip wear test simulator with the specimen at the soaking station. By comparing the amount of wear between these 2 specimens, it is possible to understand the amount of wear rate caused by friction from mechanical motion alone.^{4,18,19}

There are three rotary movement motors, and one is used on the Z-axis movement motor in the main system of the hip implant wear test simulator, and the soaking station is implemented into this system with one motor. The soaking station has the same linear movement and hardware setup. The single-axis precision control of the system with a servo motor is used in Figure 3. The force is controlled by communication between the load cell (force sensor) and the servo motor.

The motor and driver of the soaking station use the same brand as the simulator's main system, so it allows synchronous movement easily even including 3 rotary motors of the simulator with modifications in their encoders. For synchronous movement, a virtual driver in the program is used as a master to make all motors work synchronously. The force sensor measurement is compared with the output of the force parameters simultaneously on the soaking station. Integrating safety features into the control system to prevent excessive force, limit joint range of motion, and ensure user safety.

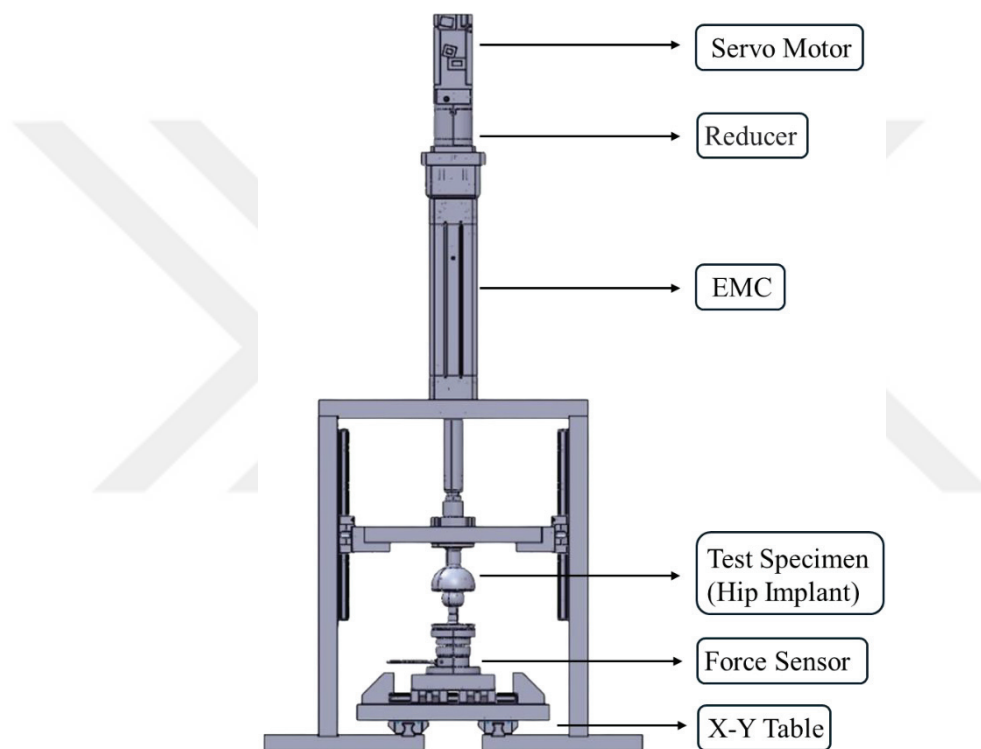


Figure 3: Design of Soaking Station Mechanism.

In addition, accessories for the simulator, a peristaltic pump, and a thermocouple circuit were acquired to circulate simulated bodily fluid via a container (gaiter) for wet-wear tests. Moreover, for wet friction tests, a pump unit and thermocouple circuit for circulating simulated body fluid with a container have been manufactured and tested as an accessory to the simulator.

Some issues occurred when the three rotary motors had trouble communicating with different brand drivers at the hip simulator, resulting in a communication error. It

was resolved by changing the existing encoders for SZE type Single Turn – Endat 2.2 encoders to solve this issue. A practical solution is applied with an order for new encoders to be delivered. Compatible encoders were replaced and sensors to set the origin points were placed onto the machine. Because the motors are downgraded to incremental motors from absolute motors. The process involved coming up with experimental solutions. Fortunately, the encoder issues were successfully resolved allowing the motors to be effectively controlled via the driver. Integration stages were carried out on the control side of the hip joint simulator with the integration of hardware, software, and control algorithms. Calibration, verifications, and integration with the mechanical system were carried out to ensure the successful completion of the project.

The alignment processes and calibration of the machine home positioning have been successfully implemented following the specifications of the project. This is achieved by precise alignment of the machine's components to predefined reference positions. Correct execution of the starting position is crucial for subsequent operations. These calibration and alignment processes are the most basic mechanical factors that can affect the simulation results to reach the ISO standards.^{2,12,15,20}

This chapter mentioned general information about the concept of the manufactured soaking station which is an accessory device for hip joint implant wear test simulator. In the chapter, it is mentioned what is needed for a soaking station and what has been completed.

In the next chapter, a literature review is conducted and briefly mentions the hip simulators and soaking station research and some general parameters to use. It shows mostly why is a soaking station needed. It is needed for comparison of the test results and the hip simulator cannot be trusted without it.

The method and materials chapter, mentions the detailed design and parameters of the soaking station, the manufactured and purchased components, control over the main system with the hip simulator, and how to handle calibration of home position and saturated electrode for real simulation.

In the result and discussion, it is mentioned about some problems with solutions and current states of problems. The discussion briefly over a numeric analysis for the potential critical part due to the applied force mechanism in Ansys.

In the last chapter, this thesis describes how to contribute to the development of a system that simulates realistic movement and wear conditions for hip implants by

collecting data that can be used to optimize implant designs and ensure compliance with international standards.



CHAPTER 2

LITERATURE REVIEW

The development of total hip replacements has significantly improved over the years, and much of that improvement was driven by an understanding of the biomechanics of the gait cycle. In this regard, the gait cycle forms an integral part of the biomedical field in general and wear rate testing simulators for hip implants, since it is used to replicate the loading conditions experienced by the hip joint during walking.²¹ Such a gait cycle, with definite, distinct phases of stance and swing, leads to repetitive loads and motions that the hip joint must endure; thus, this constitutes an important concern for hip implant wear testing and evaluation in the biomedical field.²² Wear test simulators are important laboratory equipment that provides complex motion and force patterns occurring at the hip joint during walking. These are usually sinusoidal, having been developed from the periodic motion and forces of the gait cycle for a laboratory-based simulation of the hip joint implant wear characteristics.¹³ These simulators replicate not only flexion, extension, and rotational movements but also apply loads corresponding to body weight during walking rather than realistic wear tests.²³

In vivo, data collection techniques, such as the measurement of forces and moments acting on the hip during movement, have contributed significantly to the design of modern hip joint implant wear test simulators.²⁴ These simulators can simulate the complex RoM of the human hip by implementing robotic arms in closed-loop control systems. The open robotic arm allows the reproduction of fine movements while the closed-loop control maintains this with minute adjustments to conform to the desired motion pattern. The "home position" cannot be overemphasized in these simulators, as it forms a reference from which all movements are made.²⁵ Each test from the simulator starts from a correct home position; therefore, wear testing results are less variable, which is critical for hip implants that are being bench-tested for their wear performance. If the prosthesis is set at an incorrect alignment, or if it has become dislocated during testing, either artificially high wear rates or even implant surface damage may occur, so it has been mentioned in the literature, where the exact simulator control and application of force are emphasized.

ISO-14242-1 and ISO-14242-2 define the environmental conditions, including temperature and fluid composition, which are important in wear testing simulations.^{2,3,26} These conditions are designed to simulate the physiological environment of the hip joint in the human body so that the wear results in the wear test using kinetic and kinematic data from in vivo measurements in laboratory tests can be accurately compared according to the quality of ISO standards.^{2,3,5}

Gravimetric analysis is one of the major wear measurements involving the quantification of material loss through measurement of the mass of a hip implant pre-and post-test. This form of analysis is very sensitive and forms one standard for implant material comparisons. The gravimetric analysis also informs on the effectiveness of wear-reducing strategies such as the introduction of advanced materials like highly cross-linked polyethylene that reportedly reduces wear rates by an order of magnitude.²⁷

The soak station provides this important function in hip joint wear testing, accounting for the fluid absorption exhibited by the implant materials. It can happen during a test that implants may absorb some amount of fluid, thus gaining weight and giving a fallacious wear measurement. The soak station does that by equilibrating the implant in a fluid bath in a bovine serum liquid before and after testing to make sure the weight change due to fluid absorption is accounted for separately from material wear. This becomes particularly important when comparing gravimetric results across different materials since different materials used in hip implants tend to change fluid uptake rates in the material.⁴ Soak stations typically operate with a one-axis load mechanism that is similar in some aspects to the load mechanisms used in hip simulators. The soak station has a single-axis loading mechanism used mainly for consistent fluid absorption testing, whereas hip simulators apply multi-axis loads to simulate the complex forces across the hip joint during a gait cycle. The similarity in design hence offers an opportunity for complementing such that data from the hip simulator and soak station can be combined to provide a comprehensive understanding of wear performance.^{20,28} More soak station data can be very relevant when comparing various materials or implant designs since this provides a guard against fluid absorption leading to misleading data regarding wear. Comparisons made are hence better representatives of the wear performance.²⁹

In conclusion, the incorporation of hip joint implant wear test simulators and soak stations is very important for an accurate estimation of hip implants. This hip joint implant wear test simulator replicates the complex biomechanics of the gait cycle, and the soak station provides fluid absorption, which could give a much better and more accurate

understanding of the wear behavior. Conformity to ISO standards and performance by gravimetric analysis further ensure reliability and comparability of results in wear testing for continuous technological advancement concerning total hip replacement.³⁰



CHAPTER 3

METHODOLOGY AND MATERIALS

Hip joint wear test simulators that comply with ISO 14242 standards are critical to ensuring the reliability of hip implant testing. Accurate force control following these standards, and the use of a secondary specimen for comparison, will ensure accuracy in the assessment of wear rates and ultimately lead to improved implant designs. The simultaneous use of the hip joint wear test simulators and the soaking stations can provide accurate calculations of hip implant wear rate measurements and higher quality standards for these tested prostheses to be placed in patients.^{3,4,14} The soaking station and the main system of the hip wear test simulator are finalized and prepared for the test. This chapter aims to show the manufacturing and integration process related to the main system and how to achieve the needed parameters which are ISO standards and activity data.^{2,3,5}

3.1. Design and Parameters of Soaking Station

According to ISO standards, the machine must be able to operate at a frequency of 1 Hz and the force values are specified in the ISO test standard. For the machine to be deemed compliant with these standards, it is stated that the maximum force value of the gait cycle and the phasing cycle time specified by ISO standards must be kept within a tolerance of $\pm 3\%$. In particular, the soaking station design was made based on the specifications and tolerances specified in ISO-14242-1.² During the design phase of the machine, the necessary equipment such as a linear actuator, load cell, and controller were selected according to these specifications. In order to provide accurate wear measurements, it is necessary to mimic the physiological conditions of the human body according to the ISO standards. The ISO standards specify that bovine serum should be used to imitate the synovial fluid of the human body as the liquid test environment and, the serum is used at the body temperature for duplicating the fluid uptake of the joints

and allowing wet wear tests like the human body. The liquid test environment should be kept at $37^{\circ}\text{C} \pm 2^{\circ}\text{C}$ according to the ISO standards. In this way, all parameters such as loading, frequency, and temperature were ensured to comply with ISO 14242-1 and ISO 14242-2 standards, and test protocols were developed for the machine according to these parameters.^{2,3}

In addition to the gait boundary conditions for the ISO 14242 standards^{2,3}, the new boundary conditions specific to the daily activities of the Turkish population were provided concerning the time values of each cycle of each motion data for the hip simulator.^{2,3,5} Similarly, only the compressive force components of the boundary conditions were calculated for the soaking station. The force input data is shown below with the maximum/minimum force values in Table 2 according to the experiments shown at Figure 1.⁵ The deviation from these values is 3% as required by ISO standards and the same for the soaking station.² The time boundary conditions are shown in the graphs below each daily activity.

Table 2: Maximum Compression Force (Multiplied by 75 kg).

Activity	Time (sec)	Maximum Amount of Force (N)	Minimum Amount of Force (N)
GAIT (ISO Standard)	1,00	3000	300
GAIT (LAB data)	1,30	2177	101
Ascending Stairs	1,60	2677	104
Asian Style Sitting	2,30	2111	742
Descending Stairs	1,40	2638	165
Obstacle Crossing	1,50	2255	106
Ruku' and I'Tidal	3,90	2755	1168
Ruku' to Sujud	4,30	1813	777
Sujud	4,30	1390	1035
Squat Lifting	2,15	2494	722
Stoop Lifting	2,60	899	2870

The fluid is called bovine serum and is used as a lubricant to replicate the physiological conditions of prosthesis wear testing in the human body. The viscosity and protein concentration of the liquid test environment are physiological conditions that affect the wear results. The serum liquid causes errors in the wear rate depending on the unstable or out-of-temperature standards of the liquid test environment.^{4,18,19} Therefore, the temperature conditions of the human body are maintained at $37^{\circ}\text{C} \pm 2^{\circ}\text{C}$ as also in the ISO standards.² Controlling the temperature of the liquid test environment is an important parameter for simulating the wear test results accurately. The temperature changes in the liquid test environment affect the viscosity of the serum liquid and the behavior of the proteins in the serum, thus causing errors in the wear results of the test specimen.¹⁹

According to the ISO 14242-2 standard used for gravimetric wear measurement methods, the components are weighted before and after the test to measure the amount of wear, and the resulting material loss is determined [3], [4]. These results can be used to investigate material selection for implant design. Both test specimens from the hip wear test simulator and the soaking station are stopped every 1 million cycles for measurement, and the weight measurements of both test specimens are compared in this way until 5 million cycles are completed for each movement cycle according to gravimetric wear measurement methods.^{2,4}

The soaking station to be developed requires a linear actuator to apply desired inputs without needing any extra parts for load distribution. It uses force input from ISO 14242 standards and daily life activities data with high precision, and it requires an encoder for positioning and a force sensor for force control. Figure 4 shows the axial force profile of the ISO 14242-1 standard. The x value defines the time as a percentage of cycle time and Y defines the load in kN in the represented graph. The maximum force shown is 3 kN. Thus, the selected linear actuator must be able to follow the force profile.²

In the system developed according to the ISO 14242-1 standard, the maximum load is 3 kN. This is the maximum force generated along the ISO standards and daily life activities data.^{2,5} Linear actuators can be selected based on force and flexibility data. The important criteria are high force controllability according to the desired standards in Table 1. It has been decided that EMC would be appropriate and chosen as a linear actuator for the design in Figure 5, which can easily meet the 3 kN force requirement in addition to its high precision and controllability features.^{2,31}

Considering the maximum force acting on the test specimen, the force is 3000 N.² The preferred EMC system is 63 mm because the load capacity of the product is 15900 N according to product catalog³¹, and the torque requirement of the selected motor is calculated as 14.1 Nm based on EMC maximum force at Equation 3.1. Here, the maximum force of the EMC is F_{EMC} which equals 15900 N, P_{screw} is the pitch of the screw, which is 5 mm in this system, and the efficiency of the system η is determined to be 0.9 based on this system. M_{max} , which is the maximum drive moment of EMC is taken into account for the torque requirement of the motor because the safety limit of EMC is less than the chosen motor. Also, taking the maximum force that the EMC can handle into the equation rather than just 3000 N as the maximum force data available creates a better design standard. It is considered that staying within the safety limits will increase the longevity used for the design purpose and it will be possible to expand further research topics by increasing the data limits.

$$M_{max} = \frac{F_{EMC} \times P_{screw}}{2\pi \times \eta} = \frac{15900 \times 0,005}{2\pi \times 0,9} = 14,05 \approx 14,1 \text{ Nm} \quad (3.1)$$

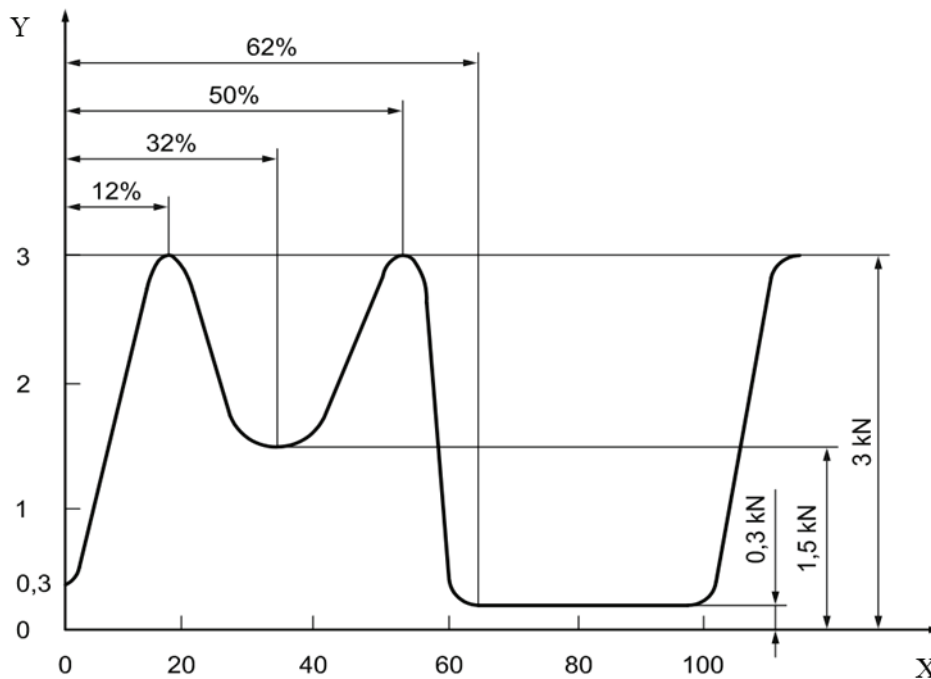


Figure 4: Force Profile According to ISO 14242-1 (Source: 2).



Figure 5: Electromechanical Cylinder.

The chosen motor has a rated torque of 0.64 Nm and a gearbox higher than 24,5 should be used to achieve 14,1 Nm according to Equation 3.2. The chosen planetary gearbox is suitable for the selected motor and meets the requirement for a gearbox size 32. The selected gearbox provides a system that exceeds the required torque. As a result, with the design of the EMC system, the preferred products remain above this stress level. The rated torque of the motor is T_{motor} which equals 0,64 Nm, the efficiency of the gearbox η is taken the same as 0,9, and r_{gear} represents the minimum required gear ratio:

$$r_{\text{gear}} = \frac{M_{\text{max}}}{T_{\text{motor}} \times \eta} = \frac{14,1}{0,64 \times 0,9} \approx 24,5 \quad (3.2)$$

The chosen EMC is capable even if the safety factor is about 3 with the maximum force value. It also has a sensitivity of 6 microns which is needed for high precision. If the critical load reaches the value of 15900 N, the maximum rod (stroke) unit is 1600 mm.³¹ It is considered that the rod of EMC will buckle after a stroke of 1600 mm at this load value. In design criteria, the maximum applied force is 3000 N from ISO standards, and even if the safety factor is taken as 3, which makes 9000 N, this is still significantly below the force limits of the chosen EMC.^{2,31} The average force within one gait cycle of ISO standards is 1627 N from the created data in Figure 4. The life cycle of the selected EMC, which is L , is found as 147673442,7 number of cycles from Equation 3.3³¹, providing 29 times the nominal utilization considering that one real test simulation for one movement is repeated 5000000 cycles. Figure 6 below shows the CAD design of the manufactured soaking station after considering these design criteria. The dynamic load

capacity of the EMC is C which equals to 17200 N, the safety factor (SF) for EMC is considered as 2, and the equivalent dynamic axial load is considered 1627 N:

$$L = \left\{ \frac{C}{F_{EMC} \times SF} \right\}^3 \times 10^6 = \frac{17200}{1627 \times 2} = 147673442,7 \text{ (Number of Cycle)} \quad (3.3)$$

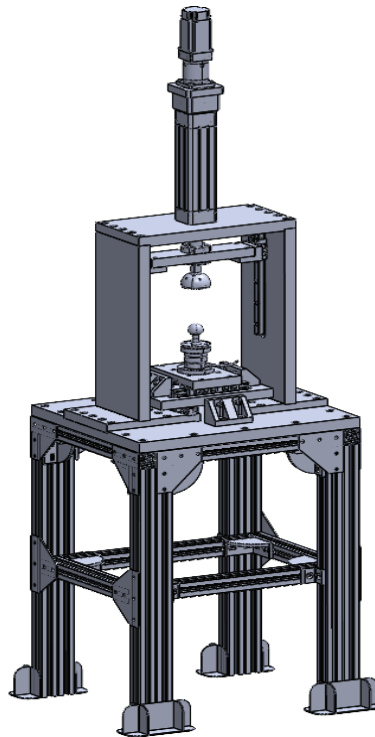


Figure 6: Soaking Station CAD Design.

The manufactured and assembled soaking station can be seen in Figure 7. While some of the parts added to the design are machined, others are bought off the shelf. Some of the ready-made parts are sleds and cars. The X-Y table is used to fix the test specimen and load cell. Also, its production consists of two parts that allow it to move in the x and y planes in Figure 8. It makes it possible to arrange manually delicate home positioning to attach the test specimen to the machine and allow examination dislocations for further research purposes.^{12,15} Other prefabricated parts are aluminum profiles. These profiles are used to make the foot parts. The upper part is made by the machining process.

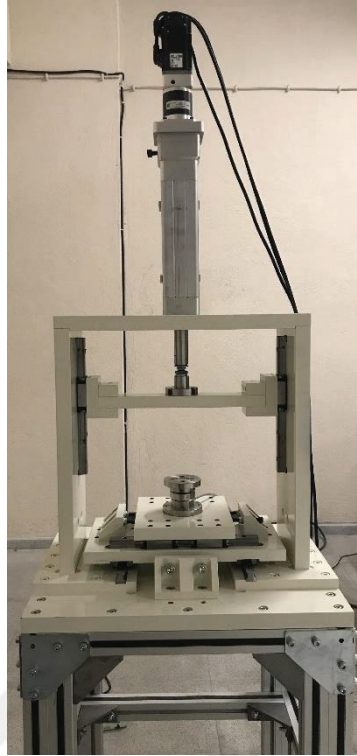


Figure 7: Manufactured Soaking Station.

A simplified force model for the hip is considered. The total hip replacement has different parts as depicted in Figure 9. The main subcomponents are the acetabular cup, liner, femoral head, and femoral stem. The hip wear test simulator aims to simulate the wear on the femoral head while the soaking station seeks to simulate the fluid uptake without wear on the femoral head. The natural femoral stem is angled shown in Figure 9, and it has a neck that may wreck due to the load applied for wear simulation. As the femoral head is an insertable part of the femoral stem, it is possible to use a straight fixture so that the femoral head tests on the acetabular cup with linear and without using the stem. It also makes the wear test more precise and sustainable when comparing results with the soaking station by removing the angle. The components of the used hip implants are according to the literature in Figure 10. The acetabular component holder, acetabular component, and plastic liner constitute the upper part of the moving part of the hip prosthesis as the acetabular cup. The cup frame is matched with the femoral head. The fixed femoral head is fixed to the load cell on the X-Y table.



Figure 8: X-Y Table Assembly.

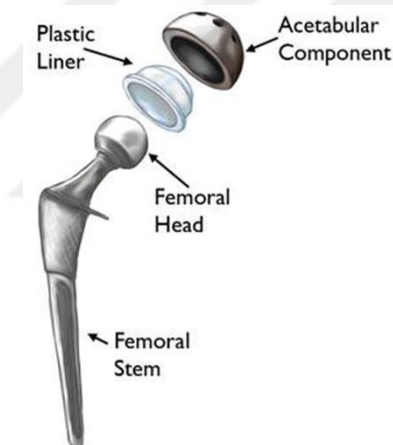


Figure 9: The Individual Components of An Illustrated Total Hip Replacement
(Source: 32).

The coordinate system of the hip implant for the soaking station is defined according to the literature in Figure 11 and the same test specimen is the TUBITAK project related to the hip joint implant wear test simulator.^{1,33} The direction of the normal force that occurred on the femoral head, which is the center of the acetabular cup is the Z-axis for the soaking station. The soaking station applies a force in the direction of one axis and all other axes are fixed for the femoral head of the test specimen.

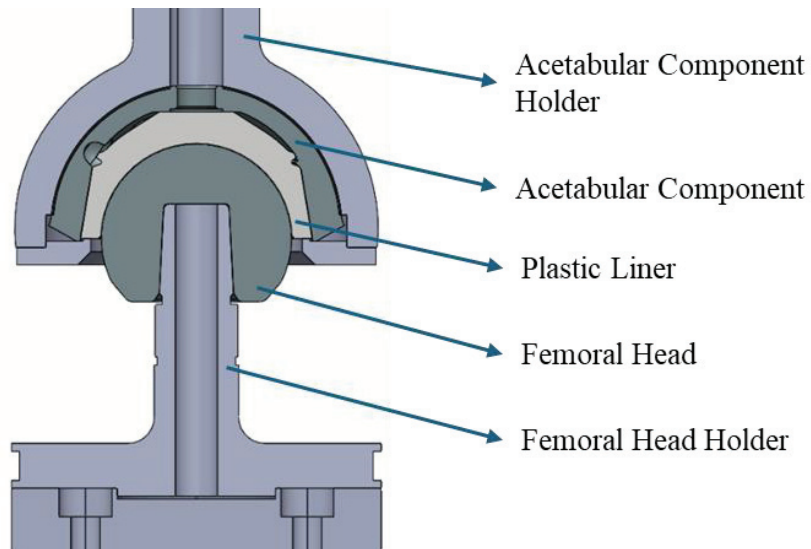


Figure 10: Components of The Used Test Specimen.

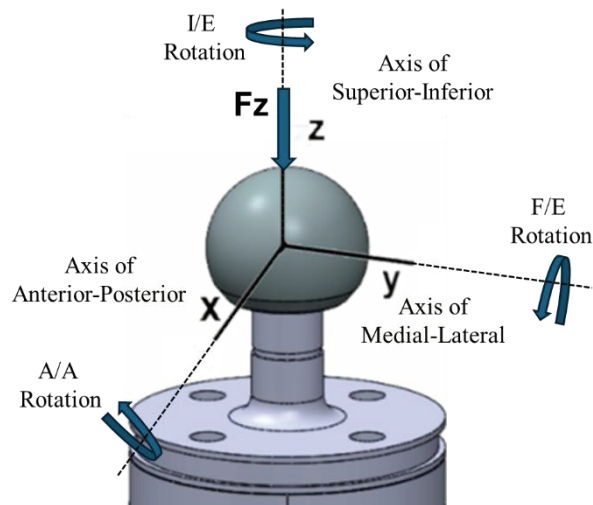


Figure 11: The Coordinate System of The Femoral Head with Jig Design.

3.2. Materials and Integration of Accessories

The operational oversight is orchestrated by the program embedded within the Programmable Logic Controller (PLC). The hip wear test simulator and the soaking

station's control hardware were successfully integrated in Figure 12. The most basic needs in the project are motors, motor drivers, CPU, PLC Enet/Ip, PMX load cell amplifier, loadcells, and a created communication network which is MODBUS as integrated hardware components. The system uses only Mitsubishi brand PLC and its modules in the hip joint implant wear test simulator and the soaking station system in Figure 13.

CPU is a PLC with 16 digital inputs and 16 digital relay outputs. It can communicate with various devices via Ethernet.³⁴ It uses the modules in Figure 12. PLC-Network Module is an Ethernet/IP module for the PLC of the Mitsubishi brand. It provides network data communication via TCP/IP, UDP/IP, and Ethernet/IP protocols and it allows communication with other devices using MODBUS ethernet protocol in the current system in Figure 12.³⁵

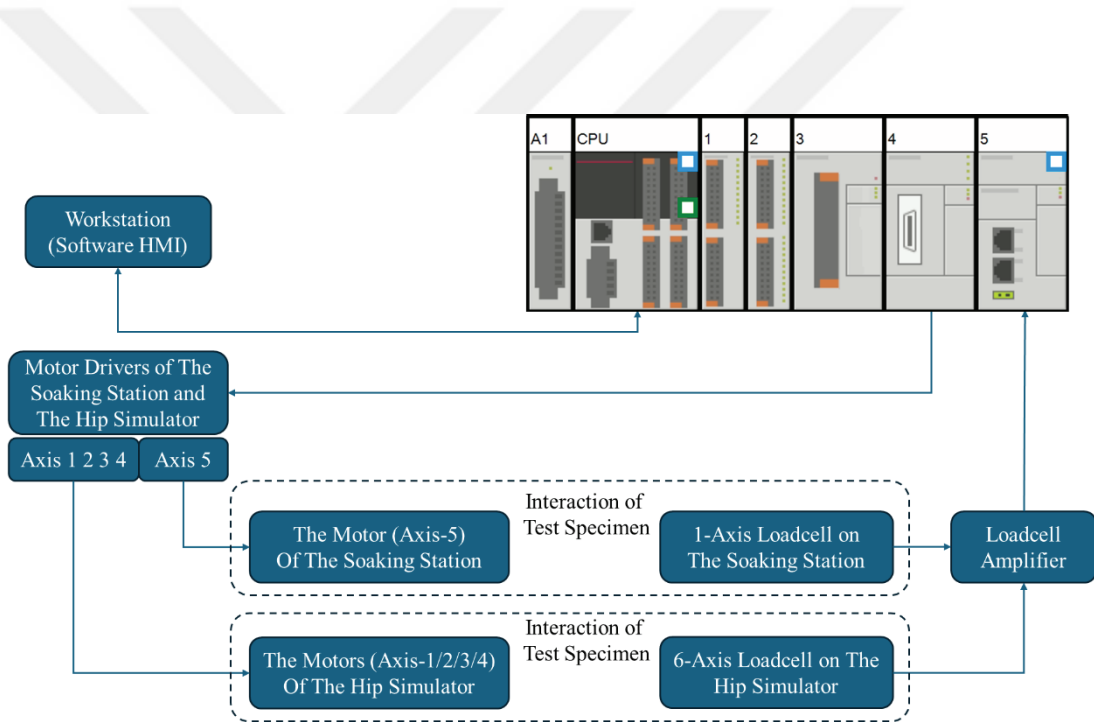


Figure 12: Integrated Hardware Components with Applied Soaking Station.

A1 is the PLC Temperature module of the Mitsubishi brand. This module converts analog signals from platinum (PT) resistive temperature sensors into digital signals. These sensors are external. 2nd, 3rd, and 4th wire connections can be made. As the number of wires increases, the resistance of the cable decreases. Thanks to this situation, more precise measurements are taken. The chosen module has 4 analog inputs to use and

temperature measurement between -100 C degree and +600 C degree with 0.5 C measurement accuracy.³⁶ Digital I/O Module with RELAY OUTPUT is the PLC input/output expansion module of the Mitsubishi brand. It has 16 digital inputs and 16 digital relay outputs.³⁷ Also, the System uses a Digital I/O Module, but it has DC INPUT as a difference. It is the PLC digital input expansion module of the Mitsubishi brand, and it has 32 digital inputs.³⁸ The Analogue I/O Module is a 16-bit resolution PLC analog input expansion module of the Mitsubishi brand. It has 8 analogue inputs. It has a conversion speed of 1 ms per channel and converts the analog signal to digital signal in 8 ms in total.³⁹ The Simple Motion Module is a specialized servo system controller module designed for PLC. It provides extended motion control capabilities and can control up to 8 axes of servo motors in synchronic control.⁴⁰ All modules are selected to be compatible with the PLC main unit.

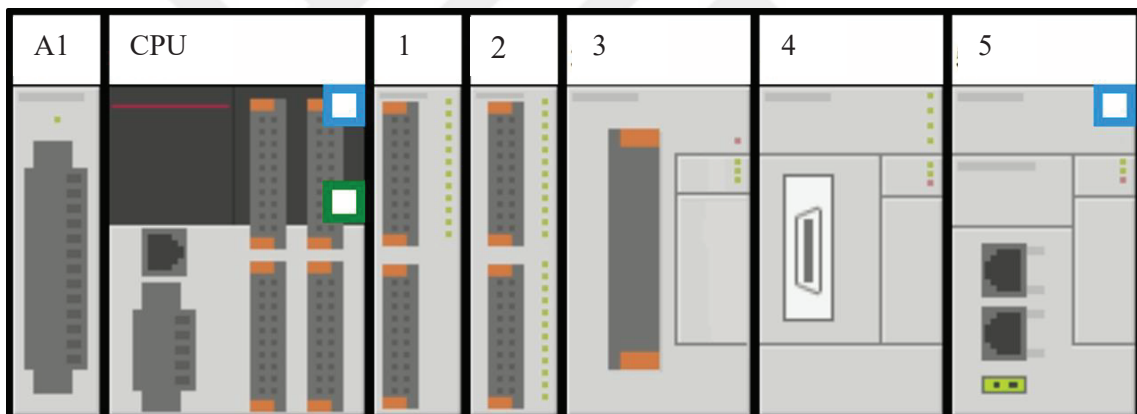


Figure 13: Used PLC Modules in The Main System of A1: PLC-Temperature Module, CPU: PLC-Main Unit, 1: Digital I/O Module with RELAY OUTPUT, 2: Digital I/O Module with DC INPUT (SINK/SOURCE), 3: Analogue I/O Module, 4: Simple Motion Module, 5: PLC-Network Module.

During the test, the communication required for the motors to perform the necessary movements (communication between the drivers) is provided using fiber cables via PLC (Programmable Logic Controller). The PLC controls the process at this point by sending force and position data to the motors through the PLC.

A communication network between brief computer, PLC, and PMX loadcell amplifier is established using MODBUS/TCP communication protocol and created a physical network environment. Two types of devices existed in a Modbus network structure. These are master and slave. Data is sent from the slave device to the master device after the Slave device receives a request for data from the master device.⁴¹ This protocol enables the real-time operation of motors with force feedback control for PID from load cells.

A HBM branded U3 load cell is preferred for this study Figure 3. HBM's rotational symmetry U3 force load cell meets high requirements for stability under lateral force by measuring ranges 0.5kN to 50 kN. The max force value is 3kN from ISO standards. The force value with a safety factor of 3 is still inside the range of loadcell measuring without problem, even if it has very sensitive measuring. Because the PID uses 1 N as sensitivity to calculate the applied force to the test specimen for meeting tolerances of 9 N from control specs of ISO standards without deviation.^{2,42}



Figure 14: U3 50kN Loadcell (Source: 42).

The system uses a Lead Fluid BT100S DT 15-44 peristaltic pump YT15 in the project in Figure 15. Peristaltic pumps provide the volume of fluid by stimulating bowel movements. With the movements it makes to provide flow, this pump prevents the liquid from touching other pump elements outside the tube and prevents any substance from entering from the outside.



Figure 15: The Peristaltic Pump (Source: 43).

3.3. Accessories of The Soaking Station

The peristaltic pump has a 25 mm hose used in the device and it provides a flow rate of 1.667 ml/min at 1 rpm. A formulation (from 1.667 mL/min to 1 rpm) is used to set the flow rate (mL/min) as the target value. Using the formula below, the RPM value we need to select from the int RPM section is calculated. For example, to provide a liquid flow of 100 ml/min at Equation 3.4:

$$\text{RPM} = \frac{\text{Flow Rate}}{1,667 \text{ (mL/min)}} = \frac{100 \text{ (mL/min)}}{1,667 \text{ (mL/min)}} = 59,99 \approx 60 \quad (3.4)$$

Lead Fluid BT100S DT15-44 is a precision peristaltic pump with a flow rate ranging from 0.007 to 380 mL/min. It can provide a flow rate in the range of 0.1-100 rpm with 0.1 rpm sensitivity. It has support for both manual and external control modes that allow fine-tuned liquid flow rate control via PLC.

Table 3 gives the nominal flow rate rates of the YT15 pump head in mL/min units.⁴³ These nominal values are for 24°C water at standard atmospheric pressure. The pipe length is 1 meter and 0.5 meters for inlet and outlet.

Table 3: YT15 Flow Rate (Source: 43).

Speed (RPM)	Tubing						
	13 mm	14 mm	19 mm	16 mm	25 mm	17 mm	18 mm
0.1	0.0060	0.0217	0.048	0.0800	0.1667	0.2833	0.38
30	1.8	7	14	24	50	85	115
50	3	11	24	40	83	142	192
100	6	22	48	80	167	283	383
150	9	33	73	120	250	425	575
350	21	76	181	280	538	992	1342
600	36	130	286	480	1000	1700	2300

A peristaltic pump in Figure 15 is purchased and tested as an accessory to the simulator, which circulates bovine serum to simulate the flow of body fluid over the test sample. In addition, a thermostat control system has been designed and manufactured for the circulation of body fluid within the body temperature range in Figure 16.

A heater resistance is embedded in a steel block and heats up from inside in the design. The steel blocks are sealed with an O-ring to eliminate infiltration in the Plexiglas cup. Thermocouples, O-ring, plexiglass, steel blocks, and delrin blocks are the list of the materials used in the assembly and manufacturing of this design in Figure 17. Steel blocks are made of 304 stainless steel for corrosion resistance in a liquid environment and easy maintenance. Plexiglas is used to keep liquid in a contained environment, and O-ring is used for sealing between steel blocks and plexiglas to prevent bovine serum liquid from flowing through this contained environment.

The thermostat volume must be higher than 500 mL for the fluid to maintain proper heat transfer in both environments according to ISO 14242 standards.^{2,3} With the

current design, the maximum volume without overflow for the liquid inside the thermostat is approximately 900 mL. Since the test specimen needs to be in a 500 mL volume of flowing bovine serum, the thermostat circulates the liquid to the test sample at a specific temperature in Figure 18. Since it is very important to keep the temperature of the serum in this system constant, a PID control algorithm is used. As a result of the PID control algorithms, a PWM signal and the necessary heating system are created. Thermocouples are used to measure the serum liquid temperature in the system. Since the thermocouple uses an analog signal, they are connected to an analog module for the PLC, and the PID block in the PLC provides the heater control with the PWM signal output. This PWM signal takes an active rate according to the degree it receives from the PID and triggers the heater resistance to operate. In the PID control, when the value increases from the desired temperature, PID gives an output as the PWM signal active rate until the temperature decreases in the fluid environment.



Figure 16: Manufactured Thermostat with Thermocouple Inside.

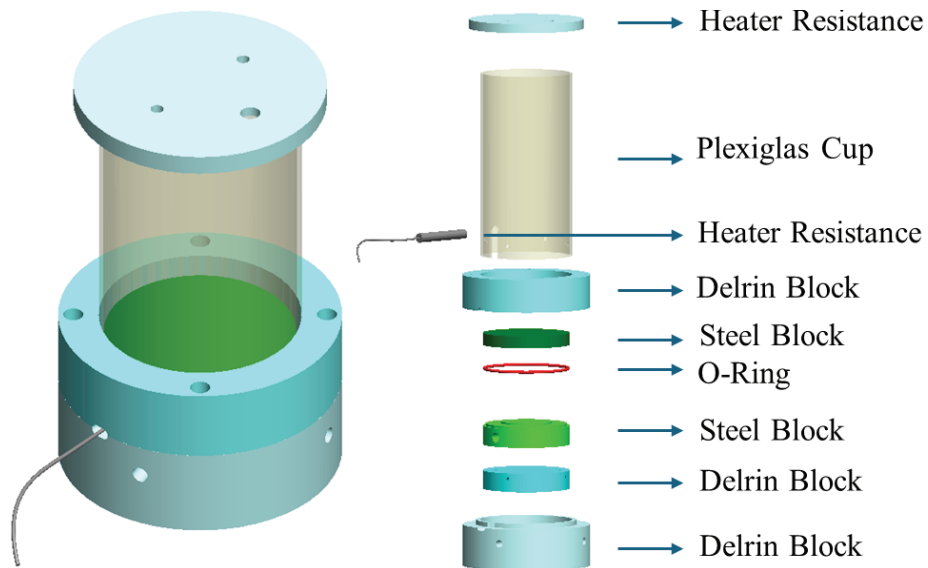


Figure 17: (Left) The Thermostat Cad Design and (Right) Individual Parts of The Design.



Figure 18: The Peristaltic Pump Used for The Liquid Circulation and The Manufactured Thermostat Assembly.

The soaking station is designed and presented in Figure 19. The control cabinet is assembled, and wiring diagrams are routed for the hip simulator. drivers, circuit breakers, and inputs and output ports are shown in the technical drawing. All drives are connected

and wired to control motors, and all have circuit breakers installed to avoid trouble with electrical circuits. The electrical system is checked for cabinet and working without any problem. The integration phase of the control side development for the hip joint wear test simulator is done successfully with hardware integration, software development, and implementation of control algorithms.

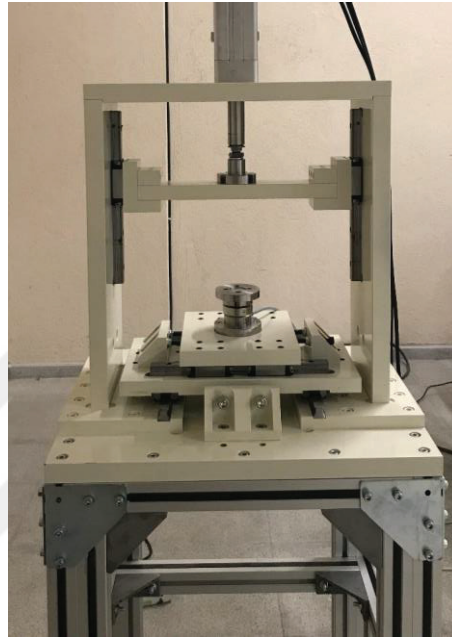


Figure 19: The Manufactured Soaking Station.

3.4. Control and Integration of The System

The implants used for testing must be simulated in real-time at the hip wear test simulator and the soaking station. The force sensor measurement is compared with the output of the force parameters simultaneously. The motors used for the hip wear test simulator and the soaking station are synchronously controlled from the same Programmable Logic Controller (PLC) and must use real-time force data from the load cells. Therefore, both the simulator and soaking station use the same PLC for synchronizing everything and creating the same environmental conditions on the test specimens. The Force/Time parameters of the ISO-14242-1 standard gait cycle and all

the compressive force cycles at the hip joint from daily life activities movements are processed with PID torque control from the workstation as HMI software. The main strategy is adding the soaking station to the subsystem of the hip wear test simulator as shown. Thus, both machines can be controlled by the same PLC and receive parameters from the same workstation to operate more synchronously on test specimens. Both the soaking station and the hip wear test simulator make the wear simulation synchronously at the same environmental conditions in the test space environment, but they are separated physically as Figure 20.



Figure 20: Physical Representation of The Manufactured Hip Joint Implant Wear Test Simulator and The Soaking Station.

While the soaking station operates only one motor for kinetic data of hip reaction forces under identical environmental conditions, the hip wear test simulator operates three motors with position control for kinematic data of hip movements and one motor controlled with PID torque control for kinetic data in the same operating system as Figure 21. The significance of synchronous operation precision in this system is highlighted for that. To conform with ISO 14242 standards, wear measurements are obtained and

compared between both test specimens every 1 million cycles of the 5 million cycles repeated in each motion simulation.² The PID torque control system regulates the compression force on the test specimen to desired force values at the time by adjusting the motor torque, using feedback data from the load cell. For this method, MODBUS/TCP communication was used in the system and a feedback force control was built between the compression force of the motor and the load cell.

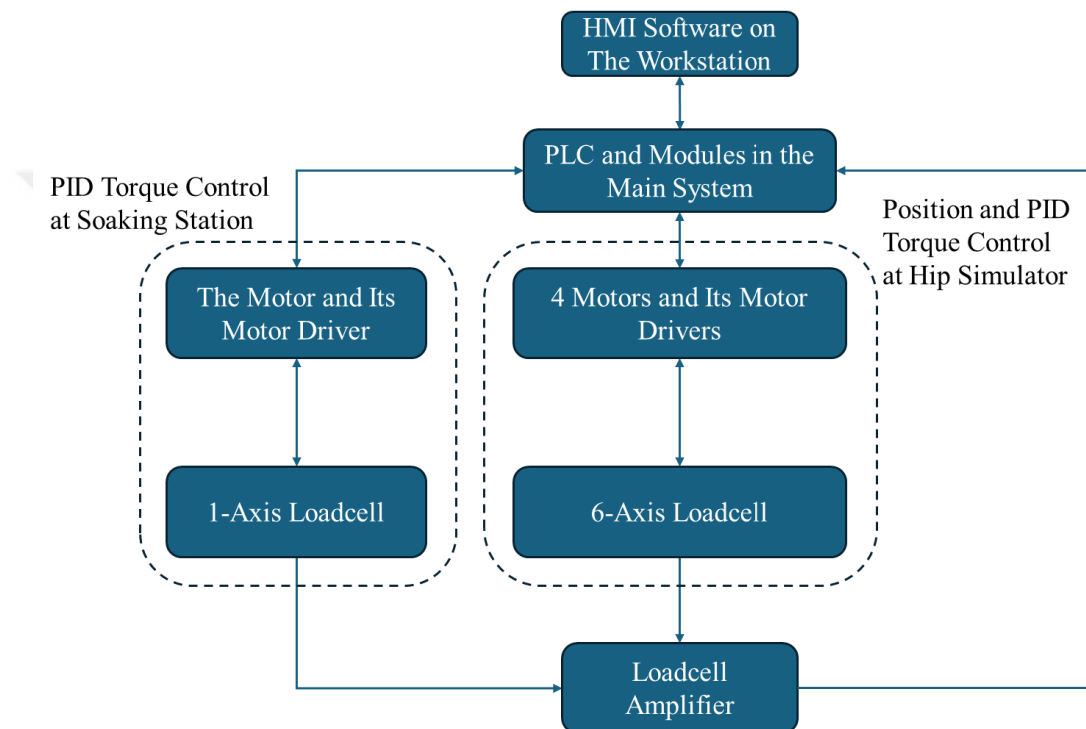


Figure 21: Schematic Representation of Motor Controls for Both Hip Wear Testing Simulator and Soaking Station.

The hip wear test simulator aims to test only the wear by hip joint movements, but the test specimen is affected by all other environmental conditions. Thus, all conditions replicated the same in the soaking station without hip joint movements that caused wear to the prosthesis to compare the results from both machines.^{2-4,16,17} The environmental condition parameters of the test environment are controlled by the PLC to comply with ISO-14242-1.² A peristaltic pump is used to mimic the human body's circulation and circulate heated bovine serum liquid from the thermostat to the test environment. The

current temperature of the serum liquid is monitored by thermocouples located at the test environment and thermostat in Figure 22. PLC turns on the thermostat to raise the test environment to body temperature at the test environment and closes the thermostat before the protein concentration and viscosity of the bovine serum deteriorate by overheating at the thermostat.¹⁹

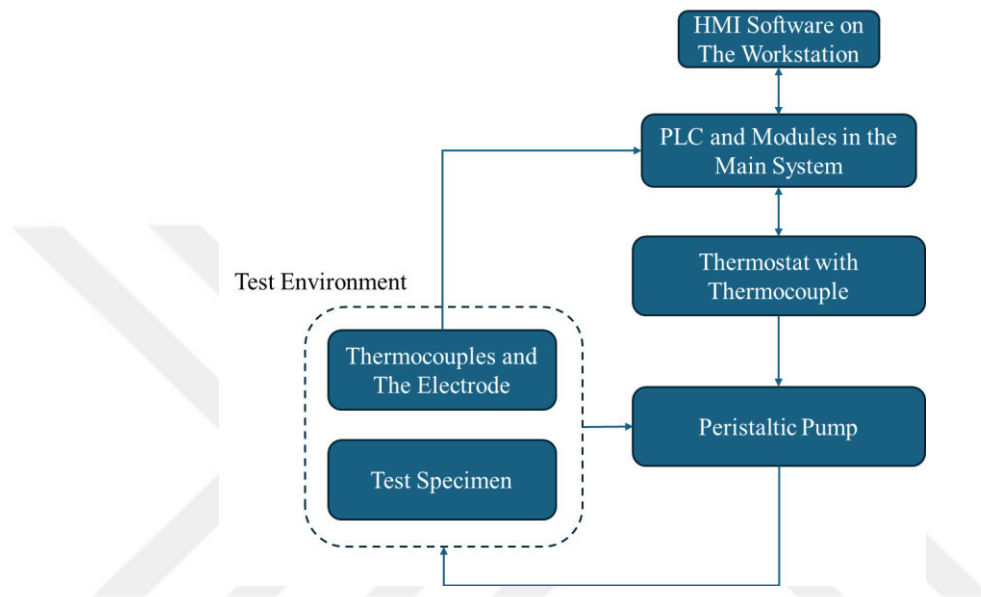


Figure 22: The Heated Bovine Serum Fluid Circulation Control for Test Environment.

The thermostat is manufactured to control the test environment which heats the serum fluid to keep it at a body temperature of $37\text{ }^{\circ}\text{C} \pm 2\text{ }^{\circ}\text{C}$ according to ISO 14242-1 standards Figure 21.^{2,4,18,19} According to ISO 14242 standards, it is designed and manufactured to be contained in a 500 mL volume liquid so that the liquid can provide heat transfer following the standards in both environments where the test specimen is located shown as Figure 23.³ The thermostat heats the serum fluid until the sensors measure $37\text{ }^{\circ}\text{C}$ in the test environment and the peristaltic pump circulates the serum fluid between the thermostat and the test environment Figure 18. The purpose of using such equipment is to ensure that the test environment closely replicates the conditions of the human body.

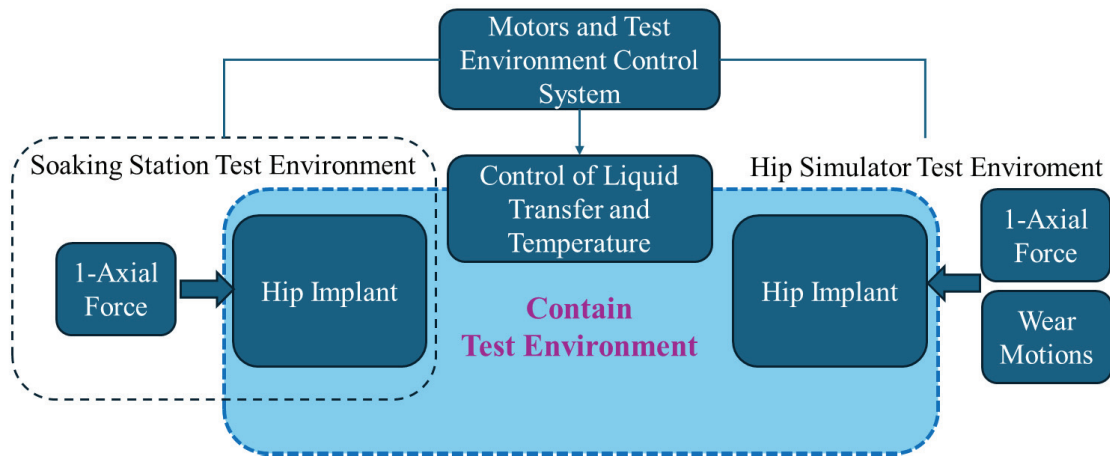


Figure 23: Test Environment Control Representation.

3.5. Software Architecture and PLC Programming

The software architecture was developed considering the need for real-time control, scalability, and adaptability. The software architecture was first controlled and validated using PLC ladder diagrams from motor tuning to the provision of initial communication on the GX Works3 program before the use with system block and the user software HMI interface in Figure 24, Figure 25, Figure 26, Figure 27, Figure 28, Figure 29, Figure 30, Figure 31. Implemented communication protocols to establish seamless and uninterrupted communication between the control side and other system components such as the motor drivers, load cell amplifier, and computer. A static IP address has been assigned to the computer, load cell amplifier, PLC, and PLC Enet/IP module (Network Module) and connected via ethernet network for establishing this physical communication environment with MODBUS/TCP communication protocol. Motors can be synchronized at any time, although one motor from the HIP simulator and one motor from the soaking station must use real-time force data from the load cells in this control system in Figure 24.

Once the PMX load cell amplifier is integrated into the PLC ethernet module, data from the load cell can be transferred in real-time to the PLC for processing as seen in the program. A Bessel analog linear filter is used on the signal from the load cell for maximum linear phase response. After calibration, the signal from the PMX load cell

amplifier is automatically regulated to 1200 Hz and the Bessel filter to 100 Hz. The data can be seen as Fx, Fy, Fz, Mx, My, and Mz from the 6-axis loadcell of the hip simulator and Fz2 from the loadcell of the soaking station in Figure 25.

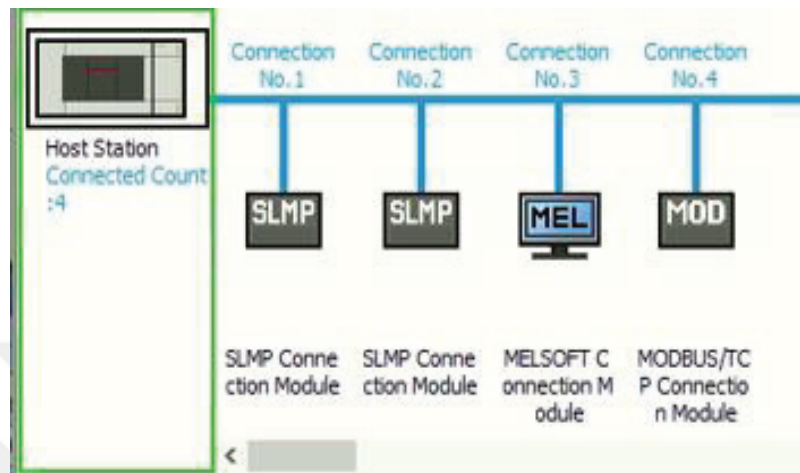


Figure 24: Physical Network Environment.

A defined maximum torque is used for protecting both the hip simulator and the soaking station. This also allows the operator to be protected in the event of sudden damage by providing a safety jolt, using the torque control mode to release the torque and stop the motors. Also, there are base stop axis buttons, and a physical emergency stop button near the operator to avoid any problems.

The PID ladder allows the PID parameters entered manually by the user to be recorded in the relevant sections in Figure 26. Parameters from the relevant device memory are used by setting the D200 parameter as in the PID ladder below in Figure 27. The PID parameter details; D90 = Given set value for force data, D92 = Measured Z-axis force value from loadcell, D200 = Storing parameters for PID, D94 = Output value to torque control. The PID ladder uses the "Word" data type range from -32767 to +32767 for the internal process, so the output value converts the torque control process parameter input value. The PID can drive the motor Z-axis motor of the hip simulator and soaking station by this method.

			FX5ENETIP_1.bS...
			R/W :EtherNet/IP communication start request(Direct)
	EMOV	U3\G12035 -0.258	F_x -0.258
	EMOV	U3\G12038 -0.499	F_y -0.499
	EMOV	U3\G12041 -0.287	F_z -0.287
	EMOV	U3\G12044 -0.392	F_z_2 -0.392

Figure 25: Read Processed Loadcell Data from PLC Ethernet Module.

	MOV	KP_2 10	D203 10
	MOV	TI_2 1	D204 1
	MOV	KD_2 5	D205 5

Figure 26: Adjusting PID Settings for Controlling Z-axis.

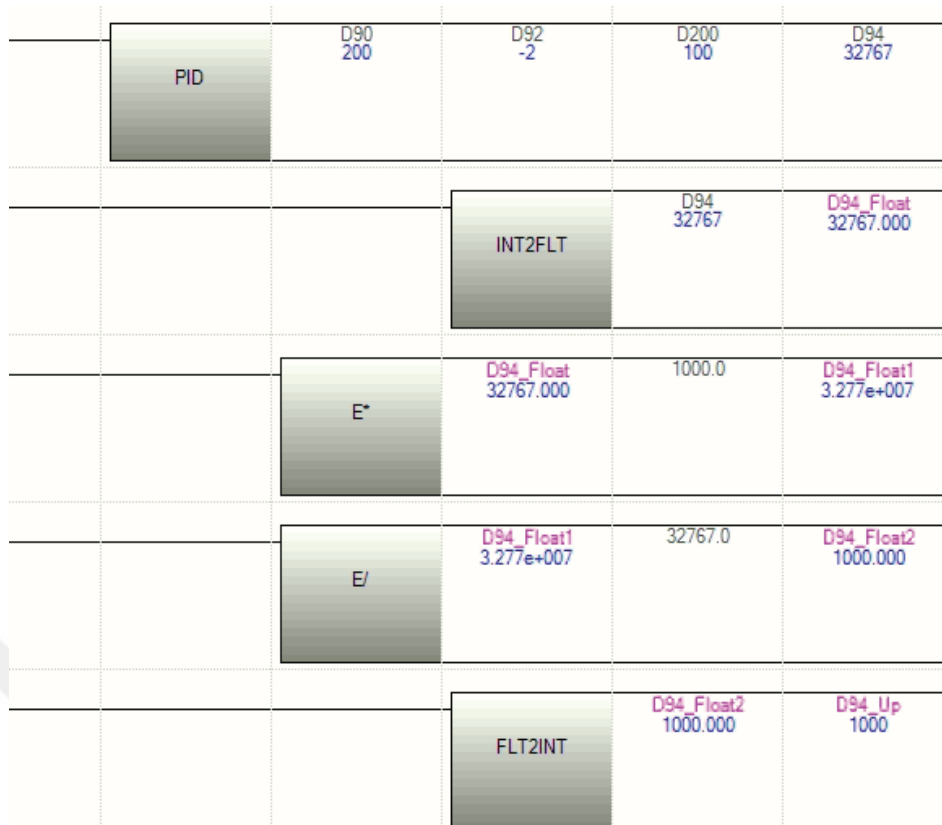


Figure 27: PID ladder for Z-axis Control.

Since the working area of the simulator is not suitable for full rotation, if it is outside the sensors when it is first started, jogging is performed before the home position. Because, when starting the home process, it is not possible to choose which direction to go home. Therefore, firstly, by making a jog operation, the operator brings the motors into the field of view of the sensor. Then the motor position is reset by performing home operation with the code in Figure 28, and then it resets again by moving to the actual starting position of the machine during operation. The operator can also control the motors by position control and apply the home process for the motors simultaneously or individually. To do this, the code uses the system blocks directly from the main control codes and no unnecessary processing is used in Figure 28. This is important when an inexperienced operator is installing and removing the test specimen before and after the simulation, and the fixture part for the homing process.

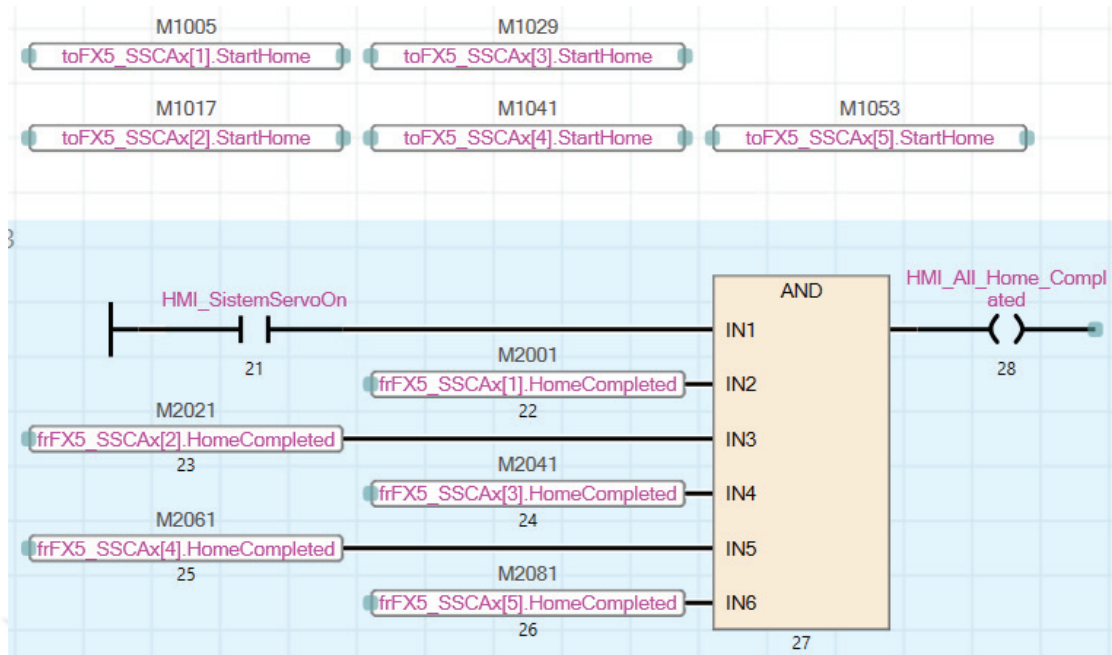


Figure 28: System Blocks of Proximity Sensors and Arranged for Homing Process.

This positioning code enables the rotation motors to be driven to the desired position by entering a degree input in Figure 29. It allows the motors to simulate the desired motion in every step from given data. This program can also be used when inserting and removing the prosthesis before and after the simulation in Figure 30.

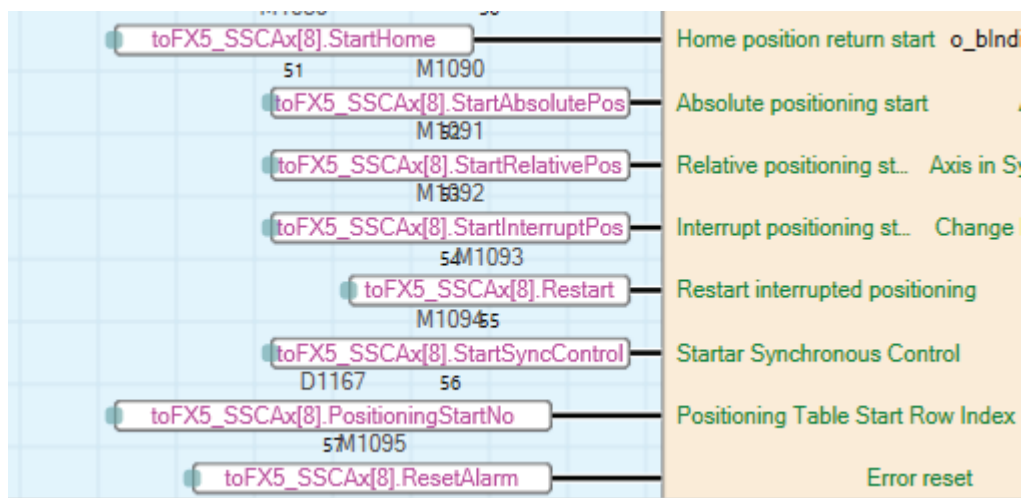


Figure 29: Positioning Code on Virtual Motor at System Blocks.

Name	Current Value
toFX5_SSCAx[2].StartSyncControl	FALSE
toFX5_SSCAx[2].JOGSpeed	0
toFX5_SSCAx[8].CmdPosition	0
toFX5_SSCAx[2].SoftLSP	0
toFX5_SSCAx[2].SoftLSN	0
toFX5_SSCAx[2].HomePosition	0
toFX5_SSCAx[2].CmdPosition	0
toFX5_SSCAx[2].CmdSpeed	0
srv_ax2_Home_Speed	360,000
srv_ax3_Home_Speed	360,000

Figure 30: Manual Input Screen for Positions and Speed Control.

It is important to create synchronous motor control to achieve quality of ISO standards.² For achieving this a virtual motor is created an Axis-8 as master and defined the one cycle time as same as wear simulation data Figure 31. Thus, all other motors in Axis-1/2/3/4/5 can easily follow the master time in Axis-8 and operate synchronously, and smooth movement can be achieved even in complex motion and force data that are difficult to become master axis.

Item	Axis #1	Axis #2	Axis #3
Synchronous control module setting	Set each module parameter.		
Main shaft			
Main input axis			
Pr. 400:Type	1:Servo Input Axis	1:Servo Input Axis	1:Servo Input Axis
Pr. 400:Axis No.	8	8	8
Sub input axis			
Pr. 401:Type	0:Invalid	0:Invalid	0:Invalid
Pr. 401:Axis No.	0	0	0

Figure 31: Arranging Master at Axis-8 and Slave at Axis-1/2/3 Synchronous Movement.

A user interface is also created from the Visual Studio 2022 community. The Program first takes the Excel data for processing in Visual Studio and the input data are arranged for all motors transfer in Figure 32. Then, the interface transferred the processed data to PLC by using MX Component programming.

A	B	C	D	E	F
Time	Axis1/ABD	Axis2/FE	Axis3/IE	Axi4/Force	Axi5/Force
00:00:00.0010000	-5.62867176952559	15.4755568549818	-9.68401641536913	-817.365423832897	-817.365423832897
00:00:00.0020000	-5.65341953859844	16.0292079069909	-9.57578832692834	-802.339939713157	-802.339939713157
00:00:00.0030000	-5.68005345073397	16.6096724830991	-9.46807462959558	-788.187551622832	-788.187551622832
00:00:00.0040000	-5.70880398794472	17.2194526327413	-9.36127016267514	-775.234062902122	-775.234062902122
00:00:00.0050000	-5.73985349413992	17.8600089844151	-9.2557946414537	-763.679904179803	-763.679904179803
00:00:00.0060000	-5.77335150104787	18.531985687158	-9.15203557721466	-753.617333189736	-753.617333189736
00:00:00.0070000	-5.80942667641947	19.2354393226145	-9.05029994813106	-745.060617295088	-745.060617295088
00:00:00.0080000	-5.84819213169474	19.9700315090726	-8.95078431433119	-737.974050096446	-737.974050096446
00:00:00.0090000	-5.8897433393553	20.7351723656587	-8.8535670071888	-732.286692031909	-732.286692031909

Figure 32: Degree and Force Data Inputs While Implementing to The PLC.

Some virtual tryouts are made to control the data and motor movements to not harm the machine and test specimens while trying new codes in Figure 33. This feature of the PLC is very important especially while working on new data from a lot of complex hip joint movement and force data.

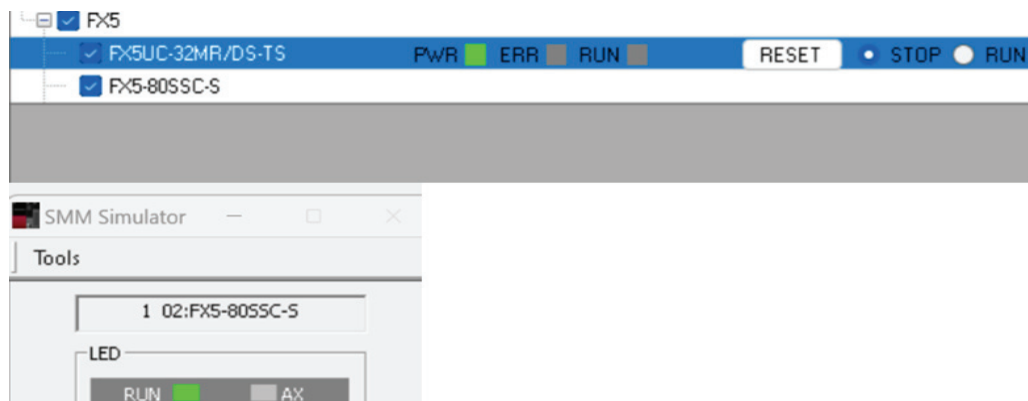


Figure 33: Virtual Tryouts in The PLC program.

3.6. Control and Integration of The System

The alignment process involves assembling the fixture within the machine at its designated home position, as illustrated in the provided image. Since this system is an open robotic arm, a specific fixture is made for zeroing the system and finding the home position in any case the system lost its home. The fixture is presented in Figure 34.



Figure 34: Fixture for HPR Operation.

The defining first home positioning process has some challenges. Because of the nature of the flexible mechanism of the open robotic arm, it needs to define both the upside and downside of the end-effectors as parallel by using the precision manufactured fixture part and creating a close robotic arm. To do this accurately, a certain amount of pressure must be given, and watch carefully the reel time data from the 6-axis sensitive Load Cell. Since the maximum value F_z is 3000N in the specifications, the pressure continues in the Z axis by using 300N, one-tenth of this pressure, for the X-Y moving table alignment process in Figure 35. While the load cell feedback gives data as F_x , F_y , F_z , M_x , M_y , and M_z , the screws of the X-Y table placed under the load cell are carefully tightened to observe and align until only the F_z variable remains. This position

is sealed for the X-Y table and the 3 motor positions of the arms' current positions were recorded to obtain the parallel position of end effectors.

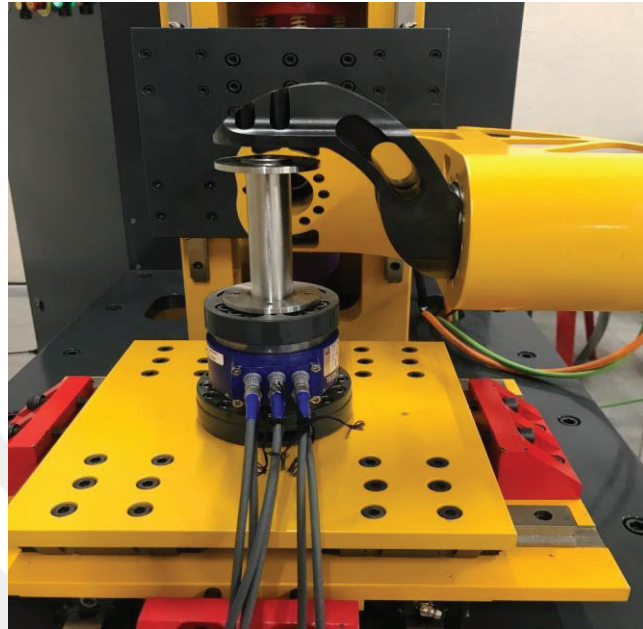


Figure 35: Representation of Aligning Fixture part X-Y Moving Table and 6-axis Loadcell.

As mentioned before, three Canis Drive motors use proximity sensors to change their encoder issues. So, the machine home position return (HPR) procedure with proximity sensors needs to be defined properly. There are some details on the program side after defining the homing placement of the motors. The motor's encoder positions are saved while in drive mode to not forget the incremental motor positions. Also, the sensors were placed at the shaft a close range of homing position. Because the workspace does not allow a full turn, and the nature of the proximity sensor can allow correct information only to reach the point encountered from one way while HPR operation. The generated code automatically jogs in the direction the user selects based on the sensor orientation and stops when the point on the shaft enters the proximity sensor's field of view before the HPR method starts in Figure 28.

Then, it starts the HPR procedure for Axis 1, 2, and 3 while it is in the sight of the proximity sensor according to the HPR method "Scale Home Position Signal" which uses

the encoder's current reading as the base location for sensitive accuracy in Figure 36. The Z-phase signal is a pulse generated by an encoder on the motor shaft. The motor will rotate during HPR operation and will only stop when this Z-phase signal is detected, allowing the system to return the servo to a known, very precise home position. The HPR operation is important and requires repeatability and accuracy. Because it ensures that the system starts where it should be every time. There are several homing methods, but this method depends on measuring the distance precisely from the point at which the sensor records the signal. Without this basic operation, it cannot be declared that it is safe, accurate, or ready to process easily as a control operation for the simulator working environment. Because it does not need to make the motor full turn during HPR operation. For axes 3, 4, and 8, the Data Set method is chosen because axes 3 and 4 are used for force control and axis 8 is only a virtual motor. With this method, the HPR will be the position where the machine HPR starts.

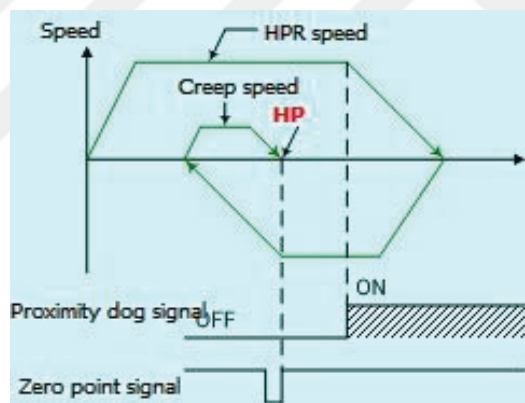


Figure 36: Scale Home Position Signal Behavior for Axis 1, 2 and 3.

After the sensors find their position for axes 1, 2, and 3, motors can make precious HPR operations correctly. This first HPR process with sensors is only used to clarify the stable position every time. However, since the required specs are in micron values and the sensors can only be placed with eye precision, this home position was shifted instead of the first home position of the motors to the position where the end effectors were previously positioned in parallel. The movement positions of the motors are calculated

according to this starting position and can be used without major deviation for the angle values used by the simulator.

Instead of placing the prosthesis and its fixtures, the focus is on aligning the machine components precisely. The values acquired during this alignment process are saved by the Programmable Logic Controller (PLC) as reference points or "home" positions. This ensures that the machine is configured accurately and consistently, serving as a baseline for subsequent operations. The use of the PLC to store these values enhances the repeatability and reliability of the alignment process during future machine setups shown in Figure 37.

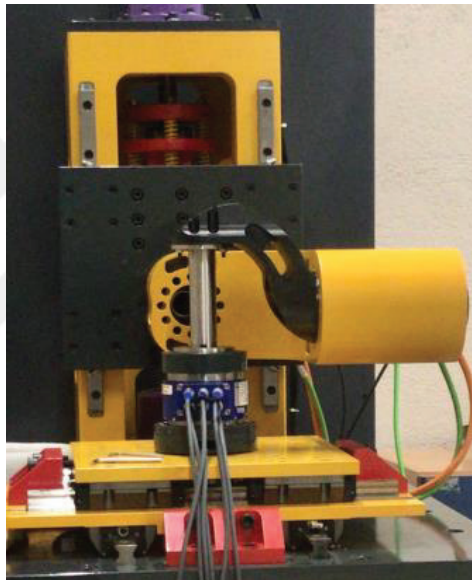


Figure 37: Home Position of Machine by Using Fixture Part.

Home positions are conducted mainly on the big arm position and small arm position of the hip simulator for this initial alignment process. This step ensures that these specific motor positions are precisely calibrated and ensures the overall accuracy and reliability of the machine's configuration.

The FARO CMM robot arm is used to measure position for the alignment process in Figure 38. Firstly, align the big arm position parallel to the machine table, and align the small arm position to this established position. These positions are measured by the CMM robot arm. The high-precision FARO CMM robotic arm was used to perform the

initial alignment, and changes in the initial positions of the small and big arms were measured in this way. This calibration step, with the help of the FARA CMM robotic arm with a tolerance of ± 0.016 mm, ensures that the starting positions of these arm positions are aligned with the required specifications. In this way, the initial position of the FARO CMM robot arm checks the accuracy of the alignment procedure and increases the accuracy of the mechanical conditions of wear simulation.



Figure 38: FARO CMM Robotic Arm.

Axes placements for alignment processes on the X-Y table for the 4 DoF hip simulator:

- Firstly, virtual planes are created in the interface of FARO CMM along the XY, ZX, and ZY axes.
- XY plane is perpendicular to above of the loadcell (The part hip prosthesis is placed). Also, it is perpendicular to the X-Y moving table located under the test specimen shown in Figure 11.

- ZX and ZY are created above the machine base that holds the robot arm.
- Set the big arm position perpendicular to the machine table by controlling the FARO CMM arm.
- The small arm position was aligned to the home position in the same way.

Incremental motor tuning:

- Since the rotational motors are incremental, proximity sensors located behind the motor shafts are used for these 3 motors of the hip simulator shown in Figure 39. In this way, the starting positions of the motors are determined.
- These sensors provide starting positions so that the motors can initiate motion and then drive to new specific positions aligned relative to the fixture part.
- In this way, the fixture position becomes the new home position, which defines the action cycle without making a full turn.

Home position verification for precise hip prosthesis placement:

- Making sure the positions of the rotational motors are aligned correctly to place the prosthesis.
- Also, the Z-axis motors are defined as home positions for both hip simulators and soaking stations by applying a load of around one-tenth of the maximum load (300N). The soaking station does not have a rotational motor, it only uses this procedure after being aligned to rotary table placement.
- After the motors are brought to the desired starting positions, the fixture part is removed by moving the motor in the Z-axis direction of the simulator using the jog operation or positioning operation.
- Using the measurements of the FARO CMM arm, move all motors to certain degrees in their work area.
- At the specified point, the newly determined home position is entered by the motors and return the motors to the starting position again.
- Setting big arm position to -90, -75, -60, -45, -30 degrees, and 0 as the home position.
- Setting small arm position to -90, -45, 45, 90 degrees, and 0 as the home position.

- Setting the Z-axis rotation motor to -180, -90, 90, 180 degrees, and 0 as the home position.
- For the linear Z-axis, move the motors -10, -5, 5, and 10 cm and return to the home position.
- After returning to these starting positions, measure the motors again using the CMM arm to ensure accuracy.

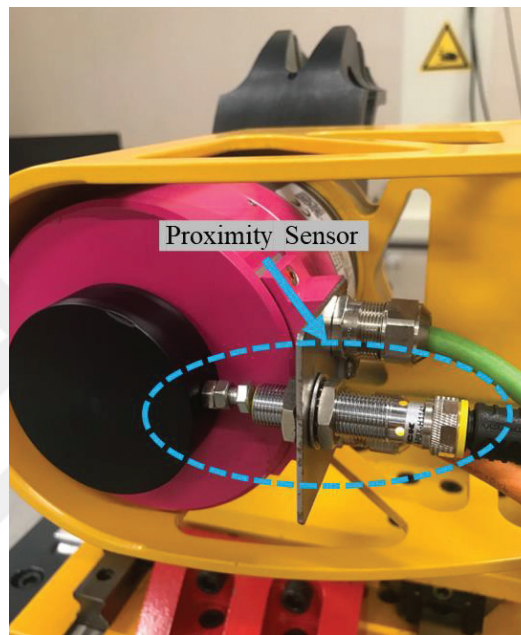


Figure 39: Proximity Sensors Integrated Behind the Motor Shafts for Axes 1, 2 and 3.

3.7. Calibration of The Electrode

An electrode should be used to measure the change in potential and the current in the test environment of the hip implant while applying cyclic compression forces inside BCS. It is important to study the fretting-corrosion on the test specimen while simulating inside BCS liquid. For this purpose, it was decided to use a SCE (Saturated Calomel Electrode) to provide a stable reference for comparison and calibration of the potentials in the solution to be measured.⁴⁴ Before using the SCE, including the calibration process, it is filled with saturated KCl solution (Potassium Chloride solution) enough that KCl

salts will settle at the bottom, see in Figure 40 (a) and should be kept in saturated KCl solution at least overnight (the beaker should also be saturated enough that KCl salts will settle, see in Figure 40 (b)). The electrodes should be stored in this saturated KCl solution. Similarly, if the precipitated crystals in the electrode completely dissolve, supersaturated KCl solution should be added to the electrode with a pipette again until the KCl salts precipitate in the electrode. This process should also be done once a month or twice as needed, by checking.

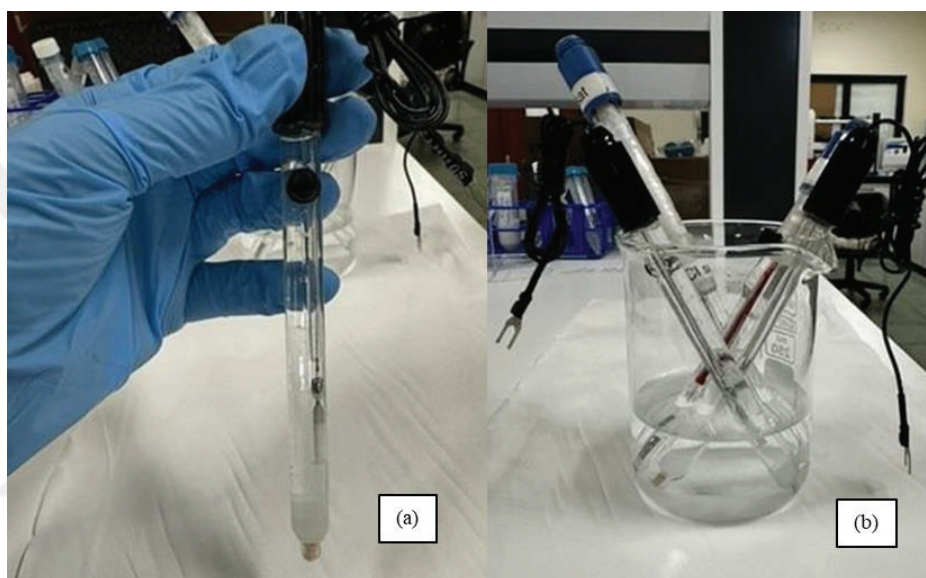


Figure 40: (a) Images of The Electrode Filled with Saturated KCL Electrolysis and (b) The Environment in Which The Electrode Is Kept.

An electrolyte with a concentration of 9 g/L NaCl is used for the calibration process; 4.5 grams of NaCl is added to 500 mL of deionized water for a total of 500 mL of electrolyte and mixed with a magnetic stirrer. The electrodes are suspended using a foot-stand shown in Figure 41. The Gamry 1010T interface device is used for the calibration process. This process requires two electrodes.

The reference electrode connection in Figure 45 (white connection) is connected to the electrode to be used as a reference, and the Working and Working sense connections shown in Figure 41 (green and blue connections, respectively); are connected to the electrode to be calibrated.



Figure 41: Electrode Calibration Setup.

The potential difference between the two electrodes is checked from the measurement device used, if this difference is not linear and high, the calibration is successful. The difference between the beginning and the end of the measuring is 0.214 mV at the end of 34 minutes from the Gamry 1010T device shown in Figure 42.

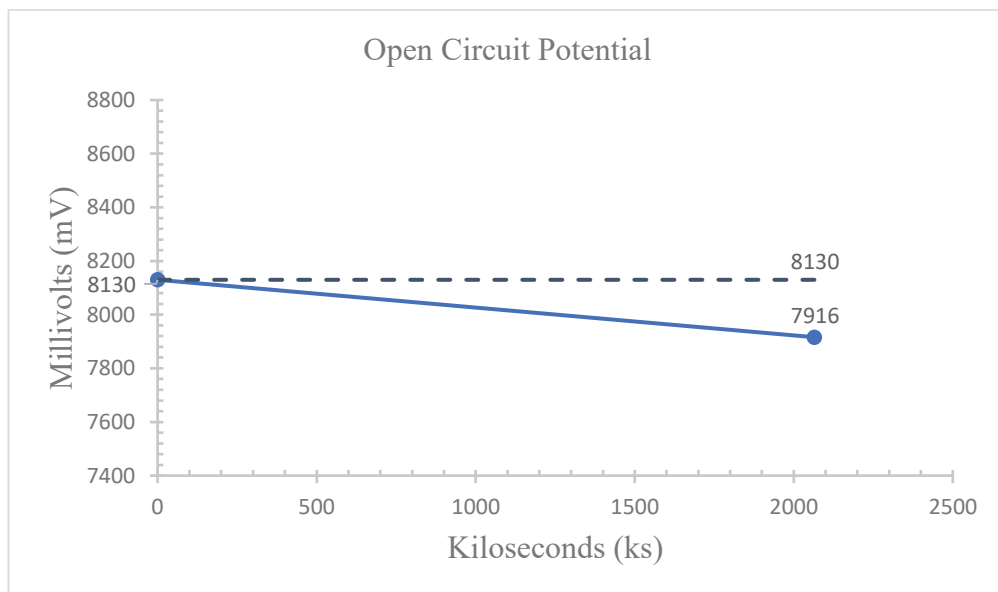


Figure 42: Measurement for The Electrode Calibration.

CHAPTER 4

RESULTS AND DISCUSSION

In this chapter, the challenges are mentioned as withdrawn of this thesis. Due to the compatibility issues with direct drive encoders and PLC in communication during integration, revision was required for the integration plan accordingly to accommodate the new components. Compatible encoders were replaced and sensors to set the origin points were placed onto the machine in Figure 43. The encoder problem resulted in ordering new products, disassembling the motors and the machine, then changing the encoders, integrating the brakes to start and stop the motors, and assembling the machine again.



Figure 43: Manual Commutation of The Servo Motors.

Testing was also performed to ensure that these combined hardware components were compatible with the intended precision. The cycle time of the PLC-Main Unit (CPU) is 34 ns. The input response time details are 10 ms and the input frequency is 100 kHz (10 us). In line with this information, unfortunately, beyond transferring the configuration from the external environment, it was not possible to do this with PLC alone at 100 ns resolution. It also works as HMI software rather than an HMI panel on the workstation. The current equipment has a 1,777 ms operation cycle in Figure 44. For this reason, a resolution of 5 ms instead of 1 ms was decided for today's equipment and the data was converted again this way by using 3 PID calculations.

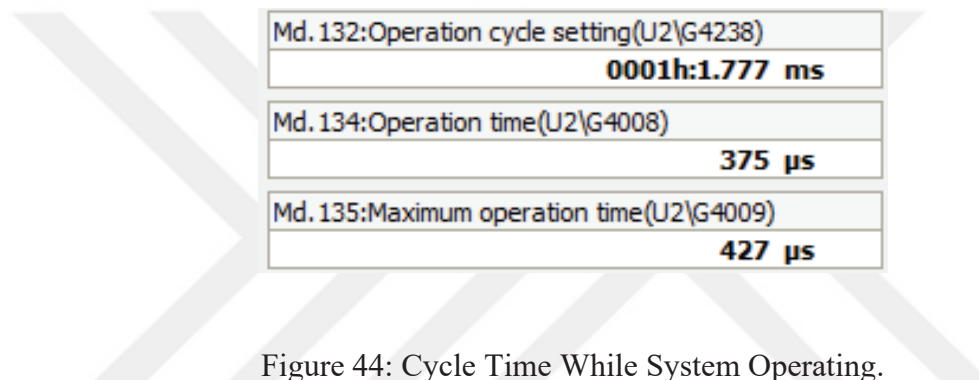


Figure 44: Cycle Time While System Operating.

A critical part of the design is estimated to be that the part holding the EMC actuator may have bent after applying force to the test specimen in the design of the soaking station. The soaking station applies compressive force as sinusoidal motion repeatedly from 300 N to 3000 N in Figure 45.

An analysis is performed for the critical bending part by the Ansys program, and the maximum sheer stress result is given in Figure 46. The mesh size was 2 mm with 115780 mesh elements after comparison results with 3 mm, 4 mm, and 5 mm mesh sizes. The max force value is 3000 N and is taken from ISO standards.² For the analysis, 3 factors of safety are considered, and 9000 N is applied for analysis to the ST37 steel block part (500 mm x 200 mm). The result shows that 39,596 maximum sheer stress on the steel block in Figure 46.

The maximum shear stress, τ_{yield} , is about half the tensile yield strength, σ_{yield} , and is 117,5 MPa for the ST37 steel material in Equation 4.1.^{45,46} This is the shear stress

limit for the elastic behavior of the steel block. If the maximum shear stress exceeds this shear stress, it means the steel block starts to deform.

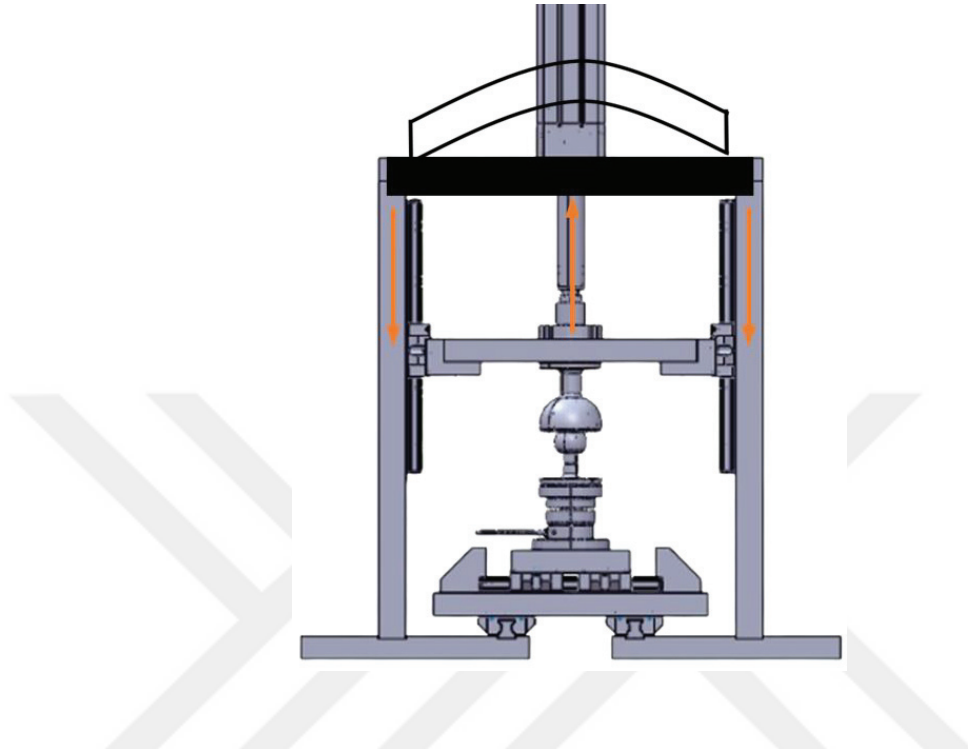


Figure 45: Bending Representation for Possible Critical Failure Component.

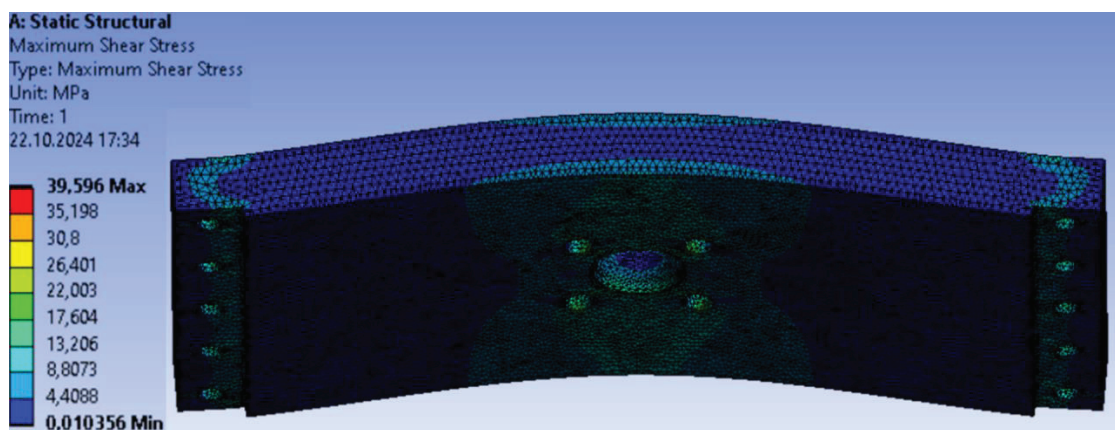


Figure 46: Maximum Sheer Stress of Critical Part at Soaking Station from Analysis.

$$\tau_{\text{yield}} = \frac{\sigma_{\text{yield}}}{2} \approx \frac{235 \text{ MPa}}{2} = 117.5 \text{ MPa} \quad (4.1)$$

The maximum shear stress is significantly lower than 117,5 MPa shown in Equation 4.1 so the steel block has not experienced any plastic deformation. This shows that the steel block can operate within safe limits without any plastic deformation.

The project has overcome challenges regarding hardware compatibility and real-time control, and the system is functioning as intended. Moving forward, the focus will be on validation and user interface enhancement.



CHAPTER 5

CONCLUSIONS

In this thesis, the physical simulators' specifications were established to replicate the actual motion of the hip implants in patients' bodies. A universal motion simulator system is programmed and merged with the soaking station. Also, PID PWM heater control allows experiments to be carried out at body temperature inside bodily fluid-containing units. Various force data can be applied to the joint thanks to the flexible interface into the soaking station. The same interactive user interface is used, which can receive flexible force and angle data so that the simulator can operate in accordance with the specifications. The soaking station's ability to operate following the specifications is examined and verified by the manufacturer. To determine the wear loss, the present implants will be tested under ISO standards.^{2,3}

The simulator device was produced within the scope of the TUBITAK 2232 project, and the manufacturability of an accessory device was covered within the scope of the AUDP project, which has been completed and physically presented in this thesis. The parts related to motor synchronizations in the main system remaining from the TUBITAK project have been solved within the scope of the AUDP project and this thesis objectives and system component approvals have been completed. This thesis's research is used for defining boundary conditions and procedures of the project according to ISO standards^{2,3} such as force, time phasing, gravimetric analysis and contain test environment conditions. According to the project's specifications, the alignment procedures and machine home positioning calibration have been executed effectively. The machine's parts are precisely aligned to predetermined reference positions to do this. For the operations that follow, the beginning position must be executed correctly for the hip implant wear test simulator and the soaking station. To meet the desired ISO standard² requirements, this calibration is the most fundamental mechanical aspect that can have an impact on the simulation outcomes.^{2,3} It is expected that with this kind of research, it will be possible to design new implant designs reliably by calculating the removed wear volume and analyzing the wear path using the soaking station as a control point for validations.

For the expectation of future technological development of the project, increasing the Technology Readiness Level from TRL 6 to TRL 9 and turning this into a product has been determined as the next target. To become a product, processes related to validation and verification are required.⁴⁷ For this purpose, another project proposal has been submitted for finalizing the product completion process and related research will continue within the scope of that project.



REFERENCES

1. Torabnia Shams; Mihcin Senay; Lazoglu Ismail. Design and Manufacturing of a Hip Joint Motion Simulator with a Novel Modular Design Approach. *International Journal on Interactive Design and Manufacturing (IJIDeM)* **2023**, *18*, 401–417. <https://doi.org/10.1007/s12008-023-01506-2>.
2. *Implants for surgery — Wear of total hip-joint prostheses — Part 1: Loading and displacement parameters for wear-testing machines and corresponding environmental conditions for test*. Iso.org. <https://www.iso.org/obp/ui/en/#iso:std:iso:14242:-1:ed-3:v1:en> (accessed 2024-10-21).
3. *Implants for surgery — Wear of total hip-joint prostheses — Part 2: Methods of measurement*. Iso.org. <https://www.iso.org/obp/ui/en/#iso:std:70668:en> (accessed 2024-10-21).
4. Estok Daniel Michael; Burroughs Brian Robert; Muratoglu Orhun Kaan ; Harris William Holmes . Comparison of Hip Simulator Wear of 2 Different Highly Cross-Linked Ultra High Molecular Weight Polyethylene Acetabular Components Using Both 32- and 38-Mm Femoral Heads. *The Journal of Arthroplasty* **2007**, *22*, 581–589. <https://doi.org/10.1016/j.arth.2006.07.009>.
5. Mihçin Şenay; Şahin Ahmet; Yılmaz Mehmet; Alpkaya Alican Tuncay; Tuna Mazhar Müslüm; AKDENİZ Sevinç; Korkmaz Nuray Can; Tosun Aliye; Şahin Serap Baydur . Database Covering the Prayer Movements Which Were Not Available Previously. *Scientific Data* **2023**, *10*. <https://doi.org/10.1038/s41597-023-02196-x>.
6. Ghalme Sachin; Mankar Ankush; Bhalerao Yogesh. Biomaterials in Hip Joint Replacement. *Biomaterials in Hip Joint Replacement* **2016**, *4*, 113–125. <https://doi.org/10.17706/ijmse.2016.4.2.113-125>.

7. Mackenzie Craig. *NHS to be banned from using “toxic” metal hip replacements after failure rate soars to four in 10 cases*. *dailymail.co.uk*.
<https://www.dailymail.co.uk/health/article-2477338/NHS-banned-using-toxic-metal-hip-replacements-failure-rate-soars-10-cases.html> (accessed 2024-10-22).
8. Müller Ulrike; Krachler Michael; Reinders Jörn; Jakubowitz Eike; Thomsen Michelle; Heisel Christian. *Determination of Low Wear Rates in Metal-On-Metal Hip Joint Replacements Based on Ultra Trace Element Analysis in Simulator Studies*. *Determination of Low Wear Rates in Metal-On-Metal Hip Joint Replacements Based on Ultra Trace Element Analysis in Simulator Studies* **2010**, 37, 23–29. <https://doi.org/10.1007/s11249-009-9486-7>.
9. Sharma Abhishek; Rai Vijeth; Calvert Melissa; Dai Zhongyi; Guo Zhenghao; Boe David; Rombokas Eric. A Non-Laboratory Gait Dataset of Full Body Kinematics and Egocentric Vision. *Scientific data* **2023**, 10.
<https://doi.org/10.1038/s41597-023-01932-7>.
10. Homes Ryan; Clark Devon; Moridzadeh Sina; Tosovic Danijel; Hoorn Wolbert Van den; Tucker Kylie; Midwinter Mark. Comparison of a Wearable Accelerometer /Gyroscopic, Portable Gait Analysis System (LEGSYS+™) to the Laboratory Standard of Static Motion Capture Camera Analysis. *Sensors* **2023**, 23, 537–537. <https://doi.org/10.3390/s23010537>.
11. Vorobyova Oksana; Horokhova Maryna; Iliichuk Liubomyra; Tverezovska Nina; Drachuk Oleksandra; Artemchuk Liudmyla. ISO Standards as a Quality Assurance Mechanism in Higher Education. *Revista Romaneasca pentru Educatie Multidimensionala* **2022**, 14, 73–88. <https://doi.org/10.18662/rrem/14.2/567>.

12. Medeiros Everton Coelho de; Ferrandini Peterson Luiz; Martins Marcelo Sampaio. Design and Evaluation of a Hip Joint Implant Wear Simulator. *International Journal for Research in Applied Science and Engineering Technology* **2021**, *9*, 989–994. <https://doi.org/10.22214/ijraset.2021.37531>.
13. Medley John Bingham. Can Physical Joint Simulators Be Used to Anticipate Clinical Wear Problems of New Joint Replacement Implants prior to Market Release? *Proceedings of the Institution of Mechanical Engineers Part H Journal of Engineering in Medicine* **2016**, *230*, 347–358. <https://doi.org/10.1177/0954411916643902>.
14. Rabbani Mohammad. *DEVELOPMENT of OPTIMAL TOTAL HIP JOINT REPLACEMENT*; 2018. <https://core.ac.uk/download/pdf/187719572.pdf> (accessed 2024-10-21).
15. Gaudin Gaël; Ferreira André; Gaillard Romain; Prudhon Jean Louis; Caton Jacques; Lustig Sébastien. Equivalent Wear Performance of Dual Mobility Bearing Compared with Standard Bearing in Total Hip Arthroplasty: In Vitro Study. *International Orthopaedics* **2016**, *41*, 521–527. <https://doi.org/10.1007/s00264-016-3346-5>.
16. *Hip Wear Testing - ISO 14242, ASTM F2025*. Lucideon. <https://www.lucideon.com/testing-characterisation/test-methods/hip-wear-testing-test-methods> (accessed 2024-10-21).
17. *Hip Simulator - ISO 14242-1*. www.endolab.org. <https://www.endolab.org/simulator-hip-implants.asp>.
18. Saha, S. Journal of Long-Term Effects of Medical Implants. *Journal of Long-Term Effects of Medical Implants* **2011**, *21*. <https://doi.org/10.1615/jlongtermeffmedimplants.v21.i2>.

19. Chee Hao Hor; Chih Ping Tso; Gooi Mee Chen. Temperature Rise by Viscous Dissipation Effect on Synovial Fluid Induced by Oscillating Motion in Artificial Hip Joint. *Case Studies in Thermal Engineering* **2021**, *24*, 100845–100845. <https://doi.org/10.1016/j.csite.2021.100845>.
20. Haider Hani; Weisenburger Joel; Garvin Kevin Lloyd. Simultaneous Measurement of Friction and Wear in Hip Simulators. Proceedings of the Institution of Mechanical Engineers, Part H: *Journal of Engineering in Medicine* **2016**, *230*, 373–388. <https://doi.org/10.1177/0954411916644476>.
21. Wade Logan; Needham Laurie; McGuigan Polly; Bilzon James. Applications and Limitations of Current Markerless Motion Capture Methods for Clinical Gait Biomechanics. *PeerJ* **2022**, *10*, e12995. <https://doi.org/10.7717/peerj.12995>.
22. Ammarullah Muhammad Imam; Santoso Gatot; Supriyono Toto; Prakoso Akbar Teguh; Basri Hasan; van der Heide Emile. Computational Contact Pressure Prediction of CoCrMo, SS 316L and Ti6Al4V Femoral Head against UHMWPE Acetabular Cup under Gait Cycle. *Journal of Functional Biomaterials* **2022**, *13*, 64. <https://doi.org/10.3390/jfb13020064>.
23. Hua Zikai; Dou Pingchuan; Jia Haili; Tang Fei; Wang Xiaojing; Xiong Xin; Gao Leiming; Huang Xiuling; Jin Zhongmin. Wear Test Apparatus for Friction and Wear Evaluation Hip Prostheses. *Frontiers in Mechanical Engineering* **2019**, *5*. <https://doi.org/10.3389/fmech.2019.00012>.
24. Mohr Maurice; Pieper Robin; Löffler Sina; Schmidt Andreas; Federolf Peter Andreas. Sex-Specific Hip Movement Is Correlated with Pelvis and Upper Body Rotation during Running. *Frontiers in Bioengineering and Biotechnology* **2021**, *9*. <https://doi.org/10.3389/fbioe.2021.657357>.

25. Zhao Honghua; Zhao Jian; Lin Yifei; Han Qifei; Cao Baolu; chen Mianpeng. Home Position and Tool Coordinates Calibration for 6-DOF Robot Based on Fixed-Point Constraint. *Journal of Physics Conference Series* **2020**, *1550*, 022027–022027. <https://doi.org/10.1088/1742-6596/1550/2/022027>.
26. Gutmann Celine; Shaikh Numa; Shenoy Satish; Bhat Shaymasunder; Keni Laxmikant. Wear Estimation of Hip Implants with Varying Chamfer Geometry at the Trunnion Junction: *A Finite Element Analysis*. *Biomedical Physics & Engineering Express* **2023**, *9*, 035004. <https://doi.org/10.1088/2057-1976/acb710>.
27. Ries Michael; Scott Marcus; Jani Shilesh. Relationship between Gravimetric Wear and Particle Generation in Hip Simulators: Conventional Compared with Cross-Linked Polyethylene. *Journal of Bone and Joint Surgery* **2001**, *83*, 116–122. <https://doi.org/10.2106/00004623-200100022-00009>.
28. Rajawat Abhinay Singh; Singh Sanjeev; Gangil Brijesh; Ranakoti Lalit; Sharma Shubham; Asyraf Muhammad Rizal Muhammad; Razman Muhammad Rizal. Effect of Marble Dust on the Mechanical, Morphological, and Wear Performance of Basalt Fibre-Reinforced Epoxy Composites for Structural Applications. *Polymers* **2022**, *14*, 1325. <https://doi.org/10.3390/polym14071325>.
29. Wight Christian; Whyne Cari; Bogoch Earl; Zdero Radovan; Chapman Ryan; van Citters Douglas; Walsh William Robert; Schemitsch Emil. Effect of Head Size and Rotation on Taper Corrosion in a Hip Simulator. *Bone & Joint Open* **2021**, *2*, 1004–1016. <https://doi.org/10.1302/2633-1462.211.bjo-2021-0147.r1>.
30. Yang Fan; Liang Yi-Wen; Shao Qiang; Li Chen-Wei; Yuan Yuan; Pan Xue-Lin; Li Zhen-Lin. [Application Value of CT Metal Artifact Correction Technology (MAC TM) in CT Review after Total Hip Replacement]. *PubMed* **2020**, *51*, 828–833. <https://doi.org/10.12182/20201160603>.

31. *Electromechanical Cylinders EMC; Bosch Rexroth Corporation*. <https://morrell-group.com/wp-content/Resources/Bosch-Rexroth-EMC-Brochure.pdf> (accessed 2024-10-21).
32. Sheth Neil Perry; *Foran Jared. Total Hip Replacement - OrthoInfo - AAOS*. [Aaos.org. https://orthoinfo.aaos.org/en/treatment/total-hip-replacement/](https://orthoinfo.aaos.org/en/treatment/total-hip-replacement/) (accessed 2024-10-22).
33. Bergmann Georg; Heller Mark; Graichen Friedmar; Rohlmann Antonius. Hip Contact Forces and Gait Patterns from Routine Activities. *Journal of Biomechanics* **2001**, 34, 859–871. [https://doi.org/10.1016/s0021-9290\(01\)00040-9](https://doi.org/10.1016/s0021-9290(01)00040-9).
34. *FX5UC-32MR/DS-TS - Mitsubishi Electric Factory Automation - Turkey*. [Mitsubishielectric.com. https://tr.mitsubishielectric.com/fa/products/cnt/plc/plcf/cpu-module/fx5uc-32mr-ds-ts.html](https://tr.mitsubishielectric.com/fa/products/cnt/plc/plcf/cpu-module/fx5uc-32mr-ds-ts.html) (accessed 2024-10-21).
35. *FX5-ENET/IP - Mitsubishi Electric Factory Automation - Turkey*. [Mitsubishielectric.com. https://tr.mitsubishielectric.com/fa/products/cnt/plc/plcf/network-communication-module/fx5-enet-ip.html](https://tr.mitsubishielectric.com/fa/products/cnt/plc/plcf/network-communication-module/fx5-enet-ip.html) (accessed 2024-10-21).
36. *FX5-4AD-PT-ADP - Mitsubishi Electric Factory Automation - Turkey*. [Mitsubishielectric.com. https://tr.mitsubishielectric.com/fa/tr_en/products/cnt/plc/analogueiomodule/fx5-4ad-pt-adp.html](https://tr.mitsubishielectric.com/fa/tr_en/products/cnt/plc/analogueiomodule/fx5-4ad-pt-adp.html) (accessed 2024-10-21).
37. *FX5-C16EYR/D-TS - Mitsubishi Electric Factory Automation - Turkey*. [Mitsubishielectric.com. https://tr.mitsubishielectric.com/fa/products/cnt/plc/plcf/io-module/fx5-c16eyr-d-ts.html](https://tr.mitsubishielectric.com/fa/products/cnt/plc/plcf/io-module/fx5-c16eyr-d-ts.html) (accessed 2024-10-21).

38. *FX5-C32EX/DS-TS - Mitsubishi Electric Factory Automation - Turkey*.
Mitsubishielectric.com. <https://tr.mitsubishielectric.com/fa/products/cnt/plc/plcf/io-module/fx5-c32ex-ds-ts.html> (accessed 2024-10-21).
39. *FX5-8AD - Mitsubishi Electric Factory Automation - EMEA*. Mitsubishielectric.com. <https://emea.mitsubishielectric.com/fa/products/cnt/plc/plcf/analog-control-module/fx5-8ad.html> (accessed 2024-10-21).
40. *FX5-80SSC-S - Mitsubishi Electric Factory Automation - Turkey*.
Mitsubishielectric.com.
https://tr.mitsubishielectric.com/fa/tr_en/products/cnt/plc/plcf/simple-motion-positioning-control-module/fx5-80ssc-s.html (accessed 2024-10-22).
41. Dutertre Bruno. Formal Modeling and Analysis of the Modbus Protocol. *Springer eBooks* **2007**, 189–204. https://doi.org/10.1007/978-0-387-75462-8_14.
42. *Data Sheet U3 Force Transducer*. HBM. <https://www.hbm.com/fileadmin/mediapool/hbmdoc/technical/B00537.pdf> (accessed 2024-10-22).
43. *Lead Fluid Catalogue*, Lead Fluid Technology. <https://sysbiosyn.ru/wp-content/uploads/2022/05/LEAD-FLUID-CATALOGUE-.pdf> (accessed 2024-10-21).
44. Manthe Jacob; Cheng Kai Yuan; Bijukumar Divya; Barba Mark; Pourzal Robin; Neto Mozart; Mathew, M. Hip Implant Modular Junction: The Role of CoCrMo Alloy Microstructure on Fretting-Corrosion. *Journal of the Mechanical Behavior of Biomedical Materials* **2022**, 134, 105402. <https://doi.org/10.1016/j.jmbbm.2022.105402>.
45. *ST37-2 Angle Steel - Low Carbon Steel For General Uses*. www.steel-sections.com. <https://www.steel-sections.com/steelsections/st37-2-angle-steel.html> (accessed 2024-10-22).

46. Ashby Michael Farries; Jones David. Continuum Aspects of Plastic Flow. *Elsevier eBooks* **2012**, 157–170. <https://doi.org/10.1016/b978-0-08-096665-6.00011-8>.

47. *Technology Readiness Level - an overview* | ScienceDirect Topics. www.sciencedirect.com. <https://www.sciencedirect.com/topics/engineering/technology-readiness-level>.

